UNIVERSITY OF OKLAHOMA

GRADUATE COLLEGE

EXTERNAL QUALITY FACTOR OF ANTENNAS AND THEIR USE IN FILTENNA DESIGN

A THESIS

SUBMITTED TO THE GRADUATE FACULTY

in partial fulfillment of the requirements for the

Degree of

MASTER OF SCIENCE

By

ADRIAN BAUER
Norman, Oklahoma
2022

EXTERNAL QUALITY FACTOR OF ANTENNAS AND THEIR USE IN FILTENNA DESIGN

A THESIS APPROVED FOR THE
SCHOOL OF ELECTRICAL AND COMPUTER ENGINEERING

BY THE COMMITTEE CONSISTING OF

Dr. Jessica Ruyle, Chair

Dr. Hjalti Sigmarsson

Dr. Justin Metcalf

Acknowledgments

I could have never achieved what I have if it were not for the constant help and support of others. I would like to thank my advisor, Dr. Jessica Ruyle, for her tireless effort in pushing me forward and helping me grapple with being a graduate student. I would also like to thank Dr. Hjalti Sigmarsson for teaching me and answering questions about the wonderful world of filters and Dr. Justin Metcalf for introducing me to the radar world and all its intricacies.

I would be remiss if I did not also mention the huge amount of students that have helped me and the friends I have made along the way. I would like to thank Clayton Blosser, Stephen Bass, Paul Winniford, Marc Thibodeau, Alex Pham, Kyle Kanaly, Ben Korty, Rosalind Agasti, and many, many others for supporting me and helping me learn and progress through my graduate studies.

Finally, and most certainly not least, I would like to thank my family for ceaselessly supporting me no matter what I chose to do. Your support, interest, and constant encouragement is what has made my journey possible.

Table of Contents

List of Figures

Abstract

Filtering antennas, or filtennas, have become a growing topic of interest in the pursuit of the minimization of the RF front end. Combining the filter and antenna, which are integral to RF front ends, allow for a decrease in the size, weight, and power consumption. In addition, a fully integrated filtenna can improve the overall performance of the RF system due to decreases in losses without sacrificing filtering capabilities. This improvement in performance is demonstrated through a noise analysis comparing a traditional RF front end utilizing a wideband antenna and an RF front end utilizing a tunable filtenna. The design of filtennas has been mostly outlined already in the existing literature and is achieved through similar methods to filter design. However, the existing filtenna literature has very little discussion on the external quality factor of the antenna, a parameter that is important to obtaining the correct desired bandwidth and correct desired response of the structure. The discussion of this topic is expanded upon in this work, and in doing so another method for finding this parameter is presented. Other methods for finding the external quality factor of antennas can also be applied from the antenna literature once the relationship between the external quality factor in filter design and the external quality factor of an antenna is understood as is presented in this work. An example second-order tunable filtenna covering all of S-band is simulated and fabricated to validate the ideas presented.

Chapter 1

Introduction

The radio frequency (RF) environments of today are typically crowded and densely packed with competing signals. There are only a finite number of frequency bands allocated for certain tasks with a growing number of devices and systems trying to access this limited frequency spectrum [1]. This has lead to increasing efforts to make more efficient use of allocated frequency, resulting in many systems in close spatial proximity using frequencies in close spectral proximity. As such, a large concern of many RF systems is the management of noise and interference. The management of these parameters can be achieved in a variety of ways, but an almost universal approach is the use of hardware filters. These filtering measures can be even more important in more hostile frequency environments with other RF systems trying to overwhelm desired signals. Since hardware filtering is so prevalent and necessary in modern systems and devices, the desire to combine them with another universal component, the antenna, is clear.

Filtering antennas, or filtennas, are a growing topic of interest for a wide variety of applications that make use of an RF front end. The RF front end refers to all of the components in a system that deals with the signal at its original RF frequency. This includes the antenna, one or more filters, the low noise amplifier (LNA), and the mixer tasked with down-converting the RF signal to baseband or an intermediate

frequency (IF). In some recent advanced systems, the entire system itself can be the RF front end as these systems do not contain any down-conversion. Instead, these systems rely on an incredibly high sample rate analog-to-digital converter to directly sample the RF signal [2]. In any event, the RF front end of a system and its constituent components will dictate the majority of the noise figure of the system as they compose the beginning of the receive chain.

In addition, there is a strong drive towards the minimization of the size, weight and power consumption (SWaP) of the RF front end for many applications. The need for the reduction in these SWaP attributes arises partly due to the desire for mobile systems which need to be considerably smaller, lighter, and more power efficient than their more stationary counterparts. Applications include space-borne systems used in satellites where additional size and weight are incredibly costly to put into orbit though this cost is decreasing [3], as well as airborne systems where similar weight and size restrictions arise due to drag or attachment point issues [4].

Traditionally the filtering portion of the RF front end is done with one or more filters just after the system's antenna. However, depending on the needed size of the antenna and the requirements of the filter(s), connecting the filter(s) directly to the antenna may not be feasible. As a result an additional transmission line is needed connecting the antenna with the filter(s), adding additional loss very earlier on in the signal chain. An example can be seen in automotive radar used for satellite communications where a small footprint and a low profile is highly desirable, but a large number of components makes this difficult [5].

The combination of the filter component into the antenna design has very clear advantages for reducing the size and weight of the RF front end for a system. By utilizing the antenna itself as a resonator, the size of the filter can be decreased for the same given order. This means that a system with a traditional RF front end

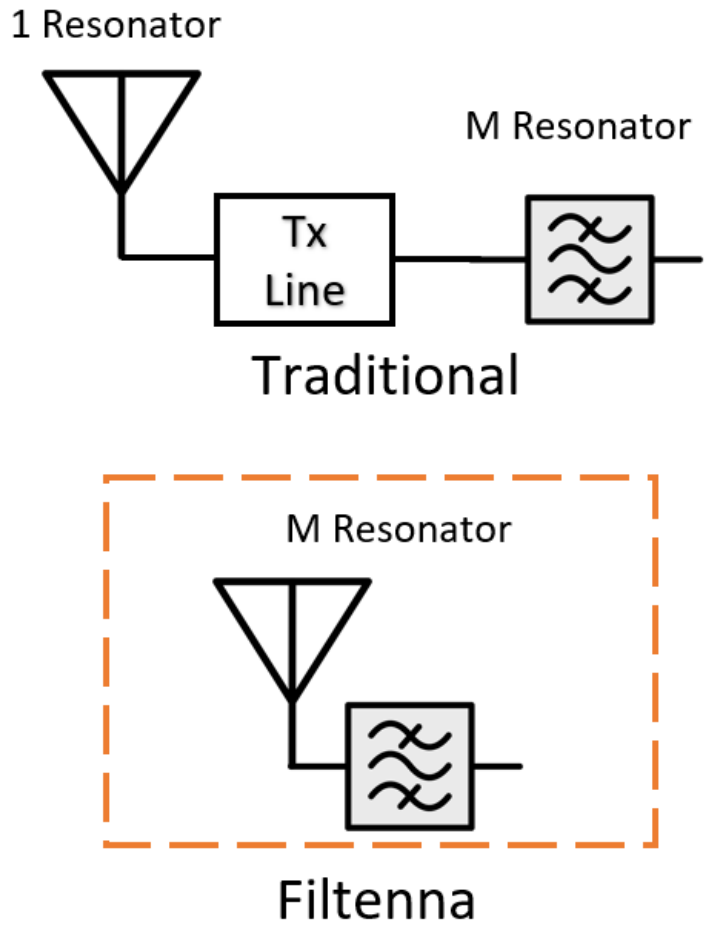

Figure 1.1: Block diagram overview of a traditional system versus a filtenna.

utilizing an M resonator filter can have the number of resonators decreased from $M + 1$ resonators to just M resonators as seen in Fig. 1.1. After this point both RF systems would look the same with a transmission line connecting this first part of the system to the rest.

There are a number of examples of filtennas that rely on modified filter designs and use the antenna as an additional resonator for filtering. For example, a filtenna can consist of two microstrip resonators with an added microstrip antenna. This will result in a third order filtering response while also being capable of radiation if the

antenna is fully and correctly integrated into the filtenna design. Using the antenna as both a means to radiate electromagnetic energy and as a resonator for higher order filtering is one of the defining characteristics of fully integrated filtennas.

1.1 Reconfigurable Filtennas

Another topic of interest for antenna design is frequency reconfigurability. Frequency flexibility allows for another option to mitigate noise and interference in a crowded or hostile electromagnetic environment [6]. If a certain portion of the frequency band is being heavily utilized or if a system is transmitting close by with a large amount of power, a frequency reconfigurable RF front end can allow for a system to change its operating frequency, decreasing the impact of the congested environment on the performance of the RF system. The tunability of the filtenna also means that filter banks are not necessary, instead a single filter can be used as long as all the resonators are made tunable. This can cut down on a large portion of the size, weight, and power of an RF front end operating at multiple different frequencies. A frequency reconfigurable filtenna combines the performance improvements inherent in tunability and higher order filtering with size, weight, and power savings improvements.

Reconfigurability of resonators is primarily done through loading mechanisms. For example, the tunable filtenna showcased later in this work tunes the resonators in the design through capacitive loading. A configurable amount of capacitance loads the resonators lowering their operating frequency and allowing for operation across a large amount of frequencies. Other reconfigurable designs rely on radio frequency micro-electromechanical systems (RF-MEMS) [7], varactors [8], and many other RF switch-based designs [9]-[12]. Non switch-based designs also

exist that make use of mechanical reconfiguration of the antenna or make use of reconfigurable materials such as ferroelectrics [13]-[16].

1.2 Filtenna Literature

Filtenna synthesis methods have been proposed in the literature such as in [17]. Here the approach relies on the circuit representation of the filter and the antenna to facilitate the integration of the two as seen in Fig. 1.2. Most of the resonators in the filtenna design are represented as shunt resonators composed of inductors and capacitors with admittance inverters representing the coupling between the resonators. The inverted-L antenna used in the design is represented as a series RLC with an additional parasitic capacitance. While most of the synthesis process is sound, the portion involving the quality factor of the antenna leaves something to be desired in terms of discussion. The quality factor of the antenna that is used to correctly synthesize the filtenna and obtain the correct design bandwidth and response shape is extracted from the series circuit representation. The resulting filtenna matches the desired filtering response relatively well with a slight bandwidth mismatch between the simulated results and the measured results.

Another synthesis method, this time for cavity-based filters instead of planar filters which are more easily represented as equivalent circuits, is proposed in [18]. The authors design a four pole filter utilizing four cavities and a slot antenna. They make a point to mention that the slot antenna is functioning as a radiating element and a port of the filter, however, it seems that the antenna in this design is not operating as an additional resonator. In addition, the external quality factor of the antenna is found using an equivalent circuit, much like the previous paper. While the equivalent circuit can be fairly accurate near resonance, it lacks the flexibility

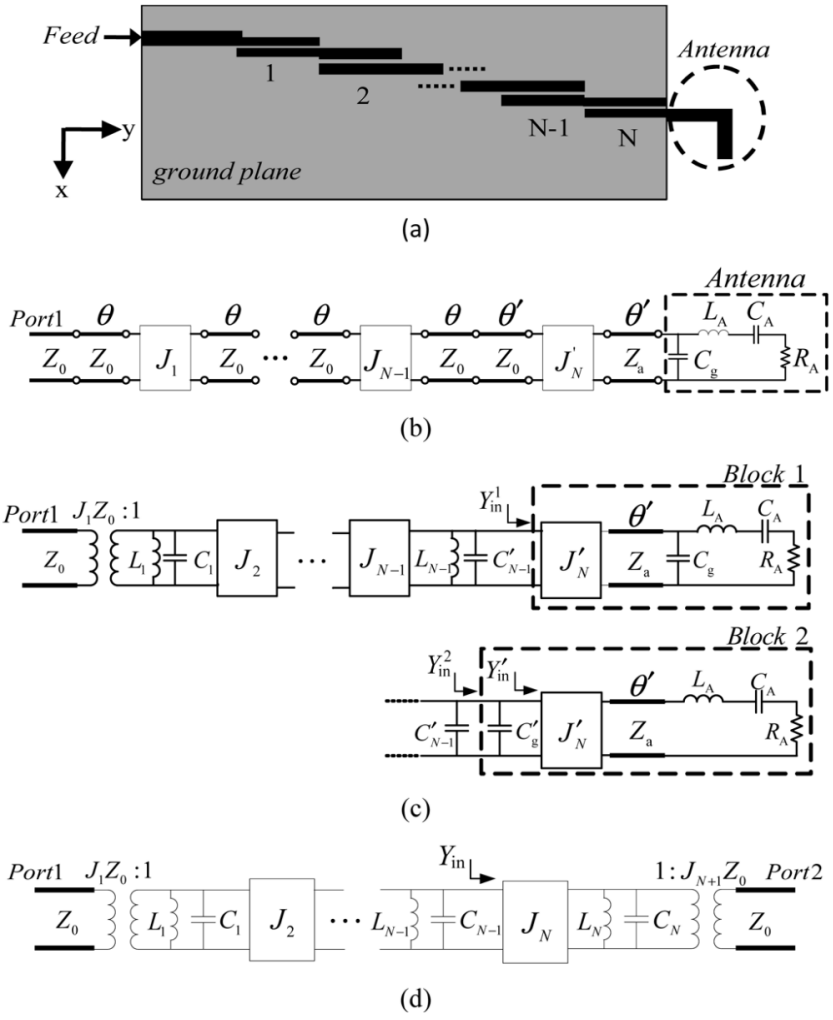

Figure 1.2: Circuit equivalent representation of the filtenna presented in and taken from [17].

of a more general method of finding the external quality factor of an antenna.

There also exist some "filtenna" designs that do not exploit the full potential of filtenna theory. This includes [19], where a tunable filtenna was made using a dual-side Vivaldi antenna and a tunable bandpass filter. Since the antenna exists only as a wideband radiating element and the filter was implemented in the feed of the antenna, the dual action function of the antenna as both a resonator in the filtering response and as a radiating structure is not being fully utilized. In addition, the

external quality factor is not discussed and, in fact, might not need to be examined in this case as the antenna is not fully integrated into this filtenna.

In addition to the literature surrounding standard filtennas, there also exists a desire for reconfigurable filtennas and recent attempts have been made to design these structures. A notable example is [20], where bandwidth control of a tunable filtenna is shown and a design procedure is laid out. The procedure points out that the external quality factor of the port side of the filtenna must closely follow the frequency dependence of the external quality factor of the antenna if a constant fractional bandwidth is desired. This design procedure includes the necessary step of calculating the external quality factor of the antenna which is done similarly to extracting the external quality factor of a resonator in a filter design. This can work, however, a different approach that leverages antenna literature can allow for a quicker and more flexible design process.

A review of the filtenna literature shows that many authors will extract the radiation quality factor of the antenna, analogous to the external quality factor, from full-wave solvers such as HFSS [17], [20]. However, this is not the case in all of the literature with some other papers extracting the normal quality factor of the antenna [21]. There are also papers that will derive the necessary external quality factors for the filter synthesis and then make no mention of it during the filtenna synthesis. In any case, a more nuanced discussion of the external quality factor of an antenna and its use in filtenna design is warranted. To the best knowledge of the author, there are no in-depth discussions on the external quality factor of an antenna that utilizes the current antenna literature to provide various methods of finding this key parameter. This may be due to the relatively new emergence and interest in filtennas which are primarily designed using a filter approach. There has been little use in the external quality factor of an antenna versus its loaded quality factor for

purely antenna applications, but the filter synthesis approach to filtennas means that this external quality factor parameter for an antenna is critical.

1.3 Outline

The objective of this thesis is to investigate the external quality factor of antennas for use in designing filtennas. The current filtenna literature makes very little mention of obtaining this parameter and what little is mentioned is extracted in a rudimentary fashion that draws heavily from filter literature. This procedure can be more fully investigated and the process can be simplified. By better understanding and deriving the relationship between the external quality factor used for resonators in filter design and the quality factor commonly used in antenna literature, a better method can be found for extracting the external quality factor of antennas for filtenna design. The derivation of this relationship, and subsequently a more streamlined approach to finding the external quality factor of an antenna in filtenna design, is presented in this work.

Additional background information on the synthesis of a filter as well as a filtenna is presented in Chapter 2. A simple method of filter design is shown involving the use of a lowpass prototype filter and a quick overview on the use of scaling and transformation techniques to modify this prototype design.

Chapter 3 of this thesis focuses on the analysis of the noise characteristics of a tunable filtenna RF system and RF systems using more traditional front ends. Included is an example comparison between a tunable filtenna system and a system using a wideband system, as well as a comparison between the same tunable filtenna system and a tunable antenna system.

Chapter 4 demonstrates the synthesis of an example second-order tunable fil-

tenna based on a 2% fractional bandwidth Butterworth bandpass filter capable of tuning a full octave in the S-band from 2 GHz to 4 GHz. This filtenna makes use of a tunable evanescent-mode cavity as the first resonator and a tunable cavity-backed slot as the integrated antenna and second resonator.

Chapter 5 involves a discussion on the external coupling of an antenna and develops a relationship between the quality factor of an antenna and its external quality factor that is needed for filtenna design. A streamlined antenna-oriented method is developed based on the input impedance of the antenna to extract this necessary external quality factor. This method is successfully applied to the cavity-backed slot antenna used in the previously mentioned tunable filtenna design. Further investigations on manipulating the external quality factor of the cavity-backed slot are discussed.

Chapter 6 presents the results for the fabricated filtenna design. The fabricated filtenna is shown to produce acceptable results, validating the design and external quality factor extraction method. Included is an overview of time domain tuning as it is incredibly useful for filtenna design and filtenna tuning.

Chapter 7 wraps up the work with a summary of the presented findings. Additional future work is proposed involving the fabricated tunable filtenna design as well future tunable filtenna design.

Chapter 2

Background

As filtennas provide the basis of this work, a solid understanding of them is necessary. This requires some foundational knowledge of filters and their design process.

2.1 Fundamentals of Filtennas

The design and use of filtering antennas, or filtennas, has recently been a growing area of research. While there are arguments to be made that a low-noise amplifier before the first filter can provide improved performance, for the majority of cases where interference is a concern, having a filter directly after the system's antenna is the superior configuration. This can prevent powerful interferers from saturating the amplifier and producing non-linearities. As such, implementing the filter and the antenna into one component can cut down on the size, weight, power, and cost of the typical RF front end among other benefits. In addition, the antenna and filter no longer need to be designed to match the standard 50 Ohm impedance and instead the filtenna can be designed with the antenna's impedance in mind. This allows for an increase in design freedom and circumvents the need for matching networks and their associated losses.

The typical filtenna is very close in its synthesis approach to a standard filter. The most important change comes in the choice of the final resonator in the filtenna design. For a filter, a standard resonator is chosen, however, for a filtenna a radiating resonator in the form of an antenna is chosen. The choice of the antenna geometry is important so that it can be easily coupled to the rest of the resonators in the filtenna design and the correct external quality factor for the given performance characteristics can be achieved.

2.2 Filter Synthesis

2.2.1 Filter Type

The design of a filter traditionally starts with some specifications: the overall role of the filter, the operating frequency of the filter, the necessary bandwidth, and the desired rejection in certain frequency ranges. From this, the filter configuration, such as lowpass, highpass, bandpass, or bandstop, is chosen. Then the type and order of the filter is chosen based on the necessary roll-off, required flatness of the passband and stopband, and phase response. A common type of filter is the Butterworth or maximally-flat filter for which the synthesis process will be explained below.

2.2.2 Lowpass Prototype

With the specifications known, the order for the desired response can be found from formulas that vary depending on the type of filter. The order is then used to construct a lowpass prototype filter that can then be easily transformed to the other filter archetypes with the correct operating frequency and impedance. This

lowpass prototype starts with a 3dB corner frequency of 1 rad/s and an impedance of 1 Ohm which can then be scaled to the desired frequency and impedance. Starting with a lowpass prototype simplifies filter synthesis and allows for a more consistent approach to various designs. This prototype is characterized by coefficients also known as lowpass prototype coefficients or g-coefficients.

The g-coefficients for a certain filter type can be generated according to their respective equations [22]. For example, the g-coefficients for a Butterworth lowpass prototype filter of order N can be generated using the equation:

$$g_r = 2\sin\left(\frac{(2r-1)\pi}{2N}\right), \qquad r = 1, 2, ..., N, \tag{2.1}$$

where N is the order of the filter. The first coefficient, $\mathbf{g_0}$, and the last coefficient, $\mathbf{g_{N+1}}$ are both equal to one for the normalized coefficients.

From these g-coefficients, simple resonators can be designed and the coupling values for those resonators can be found.

2.2.3 Filter Resonators

Simple LC resonators can be constructed directly from the g-coefficients with the normalized component values equal to the coefficient values. The filter can be constructed starting with either the shunt capacitors or with the series inductors.

However, more complex to design resonators are commonly used as they allow for significantly better performance and lower loss than discrete lumped components. The design equations for a resonator will differ considerably depending on the technology used to implement the resonator. A microstrip resonator will have to be designed differently than an evanescent-mode cavity resonator, for example. In any case, the resonator must be designed to the correct operating frequency and

will need to be fine tuned once integrated into the rest of the filter structure. External coupling and inter-resonator coupling will load the resonator slightly causing a shift in its resonance frequency which will have to be taken into account.

2.2.4 Impedance and Frequency Scaling

If simple LC resonators are to be used they can be scaled to the desired impedance and frequency. This can be completed in one step for the inductors with:

$$L' = \frac{\omega_c}{\omega_c'}\frac{R'}{R}L, \tag{2.2}$$

and for capacitors with:

$$C' = \frac{\omega_c}{\omega_c'}\frac{R}{R'}C, \tag{2.3}$$

where L' and C' are the new inductor and capacitor values, ω_c and R are the old frequency and impedance to scale from (usually 1 rad/s and 1 Ohm respectively for a prototype filter), and ω_c' and R' are the new frequency and impedance to scale to.

2.2.5 Filter Transformations

Once the lowpass prototype filter is designed, the filter can be transformed to a highpass, a bandpass, or a bandstop filter if desired. The lowpass to highpass transformation involves changing the inductors to capacitors and vice versa. This results in new component values found by:

$$L' = \frac{R'}{R}\frac{\omega_c}{\omega_c'}\frac{1}{C}. \tag{2.4}$$

$$C' = \frac{R}{R'}\frac{\omega_c}{\omega_c'}\frac{1}{L}. \tag{2.5}$$

The lowpass to bandpass transformation involves a transformation of the cutoff frequency to a defined passband. This fractional bandwidth of the passband can be defined as:

$$\Delta = \frac{\omega_2 - \omega_1}{\omega_0}, \tag{2.6}$$

where ω_2 and ω_1 are the edges of the passband and ω_0 is the geometric mean of the passband found as:

$$\omega_0 = \sqrt{\omega_2 \omega_1}. \tag{2.7}$$

The series inductor components from the lowpass prototype filter are then transformed to capacitor and inductor components in parallel with:

$$L' = \frac{R'L}{R\omega_0\Delta}, \tag{2.8a}$$

$$C' = \frac{R\Delta}{R'\omega_0 L}, \tag{2.8b}$$

and the shunt capacitor components are transformed to inductors and capacitors in series with:

$$L' = \frac{R'\Delta}{R\omega_0 C}. \tag{2.9a}$$

$$C' = \frac{RC}{R'\omega_0\Delta}. \tag{2.9b}$$

Similarly to the bandpass transformation, the bandstop transformation involves a transformation of the cutoff frequency of the filter to a defined stopband. The series inductor components are transformed to parallel inductor and capacitors with:

$$L' = \frac{R'\Delta L}{R\omega_0}, \tag{2.10a}$$

$$C' = \frac{R}{R'\omega_0 \Delta L}, \tag{2.10b}$$

and the shunt capacitors are replaced with series capacitors and inductors with:

$$L' = \frac{R'}{R\omega_0 \Delta C}. \tag{2.11a}$$

$$C' = \frac{R\Delta C}{R'\omega_0}. \tag{2.11b}$$

2.2.6 Filter Coupling

The coupling values necessary to realize the desired response, often called the coupling coefficients, can also be derived from the g-coefficients. The external coupling coefficients, usually described in terms of the external quality factor, defines the coupling strength from the resonators to the ports of the filter and are found with:

$$Q_{ext1} = \frac{g_0 g_1}{\Delta}, \tag{2.12a}$$

$$Q_{ext2} = \frac{g_N g_{N+1}}{\Delta}, \tag{2.12b}$$

where Δ is the fractional bandwidth of the filter. Typically the two external quality factors are the same as most filters are designed to externally couple to the same impedance on either side of the filter. However, when the filter is designed with two different source and load impedances, the external quality factors may not always be the same. From testing, it seems that the same external quality factor is necessary on both sides of the filtenna in order to achieve the desired bandwidth. The inter-resonator coupling, on the other hand, defines the coupling strength between the

different resonators in the filter design. These couplings can be found as,

$$k_{r,r+1} = \frac{\Delta}{\sqrt{g_r g_{r+1}}}, \qquad r = 1, 2, ..., N, \tag{2.13}$$

with r defining the resonator that is being coupled from and $r + 1$ defining the resonator that is being coupled to.

2.3 Conclusions

A simple method for synthesising filters using a lowpass prototype was presented. Modifying this lowpass prototype using frequency and impedance scaling was discussed as well as some transformations to change the lowpass prototype to a highpass, bandpass, or bandstop variant. The design of resonators and the ideal coupling values from the g-coefficients of the lowpass prototype was covered. The filtenna synthesis process follows directly from the filter synthesis process with a change in the last resonator in the typical filter design being necessary. Once the filtenna is fully synthesized, its performance in various aspects, including its noise characteristics, can be discussed.

Chapter 3

Filtenna Noise Analysis

Along with the size, weight, and power improvements that come with filtenna designs, a noticeable improvement can be seen in the overall noise figure of an RF system utilizing a filtenna instead of a separate antenna and filter configuration. Once the filtenna has been successfully synthesized, it can be compared to other RF front end solutions to analyze its effectiveness in congested RF environments.

3.1 Overall System Noise

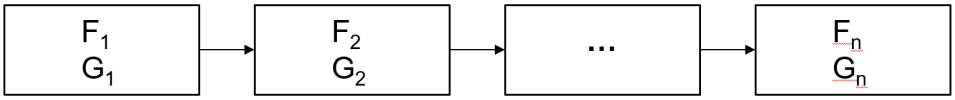

Figure 3.1: Components in cascade.

The noise figure and noise factor of a system is a measure of the degradation of the signal-to-noise-ratio, or SNR, as a signal travels through the system. The RF system under consideration is usually broken up into multiple components, each having their own noise factor and gain associated with them. This breakdown is commonly represented similarly to Fig. 3.1, with even the transmission lines that typically connect the larger components in a system being represented as their own

components. Once the system is expanded into a component-wise overview, the overall noise factor of the cascaded components is given by

$$F = F_1 + \frac{F_2 - 1}{G_1} + \frac{F_3 - 1}{G_1 G_2} + \frac{F_4 - 1}{G_1 G_2 G_3} + ... + \frac{F_n - 1}{G_1 G_2 G_3 ... G_{n-1}}, \tag{3.1}$$

where F_n is the noise factor of each individual component in the chain and G_n is the gain of each individual component in the chain [23]. The more commonly used noise figure is derived from the noise factor by

$$NF = 10 \log_{10}(F). \tag{3.2}$$

As can be seen from the equation, the noise figure and gain of the first few components of the system are responsible for the majority of the noise figure of the entire system. Usually this means that the RF front end of the system accounts for most of the noise figure, and therefore the noise figures of these components should be minimized and the gains maximized for a low overall system noise figure.

The noise figure for a passive component such as a transmission line or a passive filter or antenna is simply the inverse of its gain if the component is well matched. A more generalized form is given by

$$NF = 10 \log_{10}(\frac{T}{T_0} \left[\frac{(1 - |S_{22}|^2)}{|S_{21}|^2} - 1 \right] + 1), \tag{3.3}$$

where T is the temperature of the component and T_0 is the reference temperature, typically taken as 290 Kelvin [24]. The noise figure of non-passive components in a system are typically more difficult to characterize and are usually given by manufacturers.

3.2 Effects of Antennas on System Noise

The effects of a system's antenna on its overall noise figure is usually absent in most noise figure discussions. This is done typically as many take the noise figure to mean the degradation of the signal after the antenna, when the signal is fully contained in the system. However, since the antenna is the first point of contact between an outside signal—whether this signal is desired or not—and the system, its importance in the determination of the overall output SNR must be considered. In a traditional system, the output SNR depends on the input SNR, which in turn depends on the received power of the desired signal, the RF environment (whether it be full of noise and interference or largely quiet), and the properties of the receiving antenna. Both the match efficiency and the radiation efficiency of the antenna have an effect on the overall input SNR into the system as given by the equation,

$$SNR = \frac{\tau \eta_r S_i}{kB(\tau \eta_r T_a + \tau(1-\eta_r)T_p + T_r)}, \tag{3.4}$$

which defines the SNR a system can achieve based on its antenna, outside noise environment, and receiving system. Here τ is the antenna's mismatch efficiency, η_r is the antenna's radiation efficiency, S_i is the power of the input signal, T_a is the noise temperature of the matched and lossless antenna, T_p is the reference temperature of the system usually taken to be 290 K, and T_r is the noise temperature of the rest of the receiving system [25]. In addition to the antenna's radiation characteristics effects on the SNR of an RF system, the antenna itself can be used as a spatial filter. By pointing the main beam of the antenna at the source of the desired signal and the nulls of the antenna's radiation pattern at sources of noise or interference, the desired signal's power can be increased while minimizing the strength of unwanted

signals.

3.3 Effects of Filtennas on System Noise

A filtenna removes the loss and noise associated with two connectors and a transmission line that is usually used to connect the traditionally separate filter and antenna components. The reduction of this loss and noise near the front of the signal chain can help improve the overall SINR of the system. This reduction can be especially useful in digital phased arrays where the signals of interest can more easily be overwhelmed with noise or interference [26]. In addition, tunable filtennas allow for the avoidance of noise through frequency reconfigurability. By changing the operating frequency of the RF front end, bands with high amounts of noise and interference can be circumvented without degradation in signal strength.

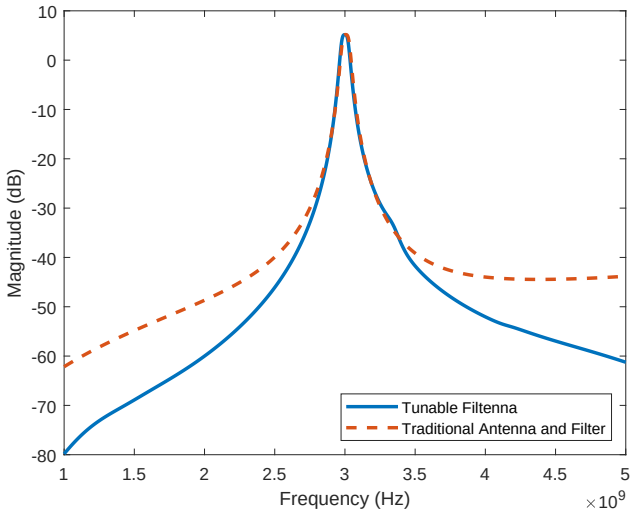

Figure 3.2: Rejection comparison between a filtenna front end and a traditional front end.

A comparison can be made between a tunable filtenna and a more traditional

wideband antenna followed by a second-order filter. The gain as seen after the first filtering portion of each system is shown in Fig. 3.2. This comparison is made due to the prevalence of wideband solutions in many situations where a tunable solution might prove better. These wideband solutions are easier to implement than a tunable solution, but this comes at the cost of increased vulnerability to noise and interference from the outside RF environment.

The wideband setup was simulated using the response of a second-order evanescent-mode cavity filter with the added gain of a 6 dB wideband antenna. The out-of-band rejection of the filtenna is indeed superior in this example. The filtenna's performance closer to the operating band is similar as both designs are based on a second-order Butterworth filter with a fractional bandwidth of 2%.

Even ignoring the other benefits, such as a decrease in loss due to the omission of connectors and a transmission line between the antenna and filter, the filtenna allows for a higher out-of-band rejection. Combined with tunability this higher rejection can lead to superior performance in noisy and interference-heavy environments. An analysis was done between the filtenna and a more traditional front end using a wideband antenna followed by a second-order evanescent-mode cavity filter. This analysis incorporated the previously discussed noise figure and antenna input SINR analysis and used a coherent interference signal at 2.8 GHz. The filtenna, wideband antenna, and filter were tuned or designed to operate at 3 GHz with the filtenna and filter having a fractional bandwidth of 2% so that the interfering signal is just outside the operating band. This setup produced the results seen in Fig. 3.3 with the filtenna consistently able to handle higher interference levels at different desired signal levels before the amplifier approached its 1 dB compression point. The ratio of the desired signal power to the interference power set the maximum SINR levels on the y-axis and the interference levels by itself can be seen on the

x-axis. In this example, the power of the desired signal is set as the maximum it can be without pushing the amplifier past its 1 dB compression point at a given interference power level. The 1 dB compression point of an amplifier refers to the point at which the amplifier's gain response falls 1 dB below it's constant rated gain. Past this point the amplifier will produce increasing amounts of non-linearities such as harmonics and distortions that can render the received signals unusable.

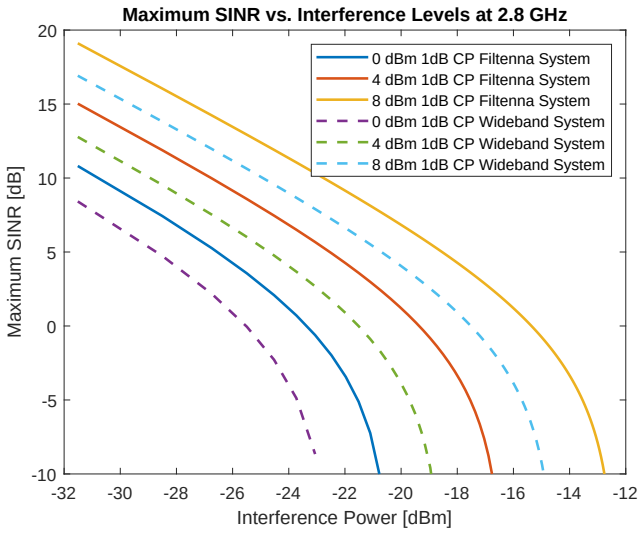

Figure 3.3: Saturation comparison between a filtenna front end and a traditional front end.

When the loss caused by a transmission line in between the antenna and filter is taken into account, the noise figure difference and loss of SINR can be seen more clearly. The amount of loss from the transmission line depends on the length of the line as well as the operating frequency and materials used in the transmission line itself. Therefore a comparison was made between two similar systems with the traditional, non-filtenna system incorporating a transmission line with differing amounts of loss between the antenna component and the first filter component. All other components past the antenna, transmission line, and filter were kept the same

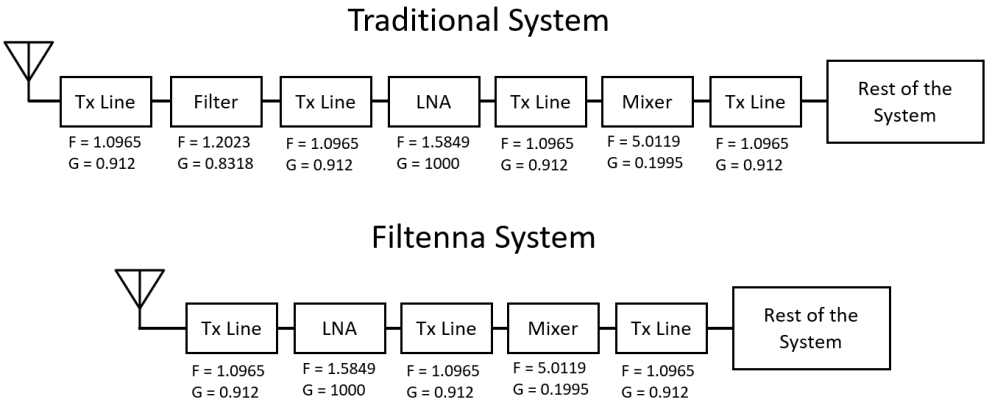

Figure 3.4: Block diagrams for the traditional wideband system and the tunable filtenna system.

for the two systems. For this reason the transmission lines past this point are omitted as both system would contain them. The block diagram for the two systems can be seen in Fig. 3.4 with each component's noise figure and gain given. Equation 3.4 was used to calculate the SNR of both the filtenna and antenna with the parameters given in Table 3.1. The wide tuning range of the filtenna leads to a more variable radiation efficiency and mismatch efficiency than the more traditional antenna. For the noise analysis, the lowest mismatch and radiation efficiency values across the entire band for the filtenna were used to illustrate the improvement the filtenna is capable of even in non ideal circumstances. A highly efficient and well matched wideband antenna was also used as a comparison point. In essence, this comparison shows a worst case scenario for the filtenna and a best case scenario for the traditional system.

The wider bandwidth of the wideband solution means more white noise deteriorates the SINR compared to the more narrowband tunable filtenna with a bandwidth of approximately 2% at 3 GHz or around 60 MHz of bandwidth. This results in the SINR difference being larger between the two systems at lower interference levels

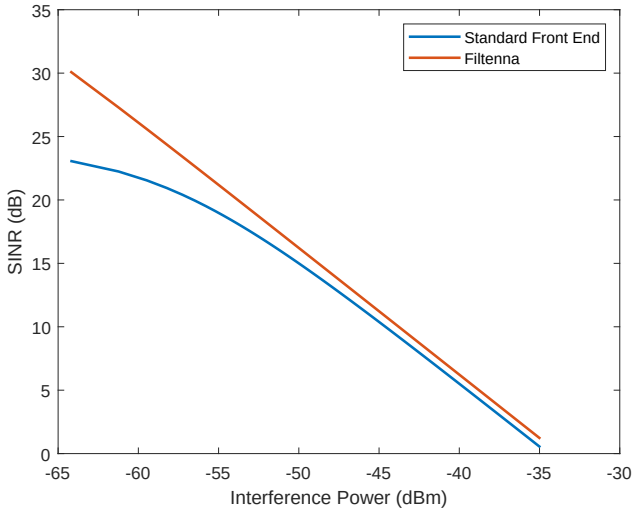

Figure 3.5: SINR comparison between a filtenna front end and a traditional wideband front end.

where the white noise plays a larger role as seen in Fig. 3.5. Another important parameter in this comparison for finding the SINR difference between the filtenna and a more traditional wideband antenna is the noise temperature of the respective antennas and the noise figures of the rest of their systems. The noise temperature of an antenna is a function of the antenna's RF environment. Therefore, assuming that both the filtenna system and antenna system are in the same RF environment with the same beamwidth, this parameter will be the same between the two. However, due to the fact that the filtenna system omits a transmission line the noise figure of that system is lower than the wideband system. The noise temperature can be found from the noise factor with

$$T = T_0 \cdot (F - 1), \tag{3.5}$$

where T_0 is the reference temperature of the component or system, typically 290 K, and F is the noise factor of the component or system.

Table 3.1: Parameter comparison between the filtenna and antenna used in the noise analysis.

System	Mismatch Efficiency	Radiation Efficiency	Antenna Bandwidth	Antenna Noise Temperature	System Noise Temperature
Wideband	0.95	0.9	2000 MHz	94.75	397.84
Filtenna	0.95	0.8	60 MHz	94.75	235.39

Another comparison can be made between a tunable antenna and tunable filter RF front end and a tunable filtenna RF front end. In this case, the difference between the two systems is significantly smaller as both radiating elements have the same bandwidth. If the rejection of the tunable filter used in the tunable antenna case is comparable to that of a evanescent-mode cavity filter, then the out-of-band rejection of the tunable traditional system and the tunable filtenna system will be similar. If the noise bandwidth and the out-of-band rejection of the two systems is similar, then any differences in the overall SINR performance between the two systems must stem from the antenna/filtenna's radiation characteristics and the overall noise figures of the systems. The elimination of the transmission line in the filtenna system will result in a lower noise figure for that system compared to the tunable antenna and tunable filter system. This will result in an overall increase in SINR for the filtenna system as seen in Fig. 3.6 if the filtenna's radiation efficiency and mismatch efficiency is comparable to that of the tunable antenna. The amount of increase in SINR is dependent on the amount of loss that occurs in the transmission line that is eliminated in the tunable filtenna case. For the results seen in Fig. 3.6 the transmission line is chosen to have a loss of 0.4 dB.

It should be noted for all the comparison cases discussed above, the gains of the antennas or filtennas were all the same. If the gains of the compared radiating

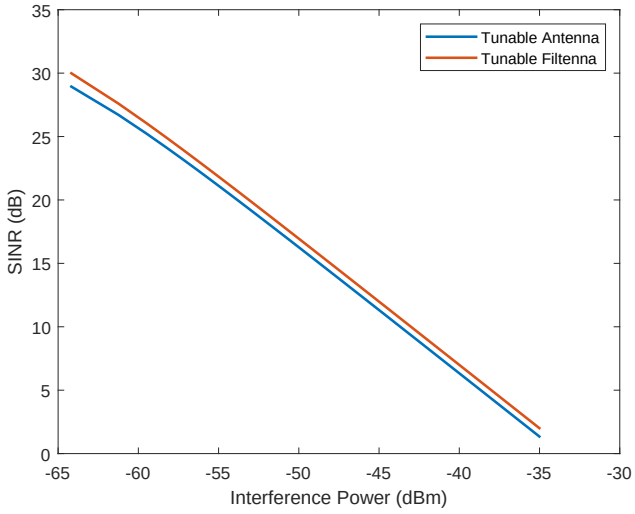

Figure 3.6: SINR comparison between a tunable filtenna front end and a traditional tunable front end.

elements, or more specifically for the receive case the effective aperture of the radiating elements, were different that would impact the spatial filtering capabilities of the RF systems. As the effective aperture of a receive antenna or filtenna increases more power is captured. In addition, the larger effective aperture decreases the radiating element's beamwidth bolstering its spatial filtering.

3.4 Conclusions

The filtenna presented in this example comparison has been shown to outperform traditional solutions to the RF front end. The filtenna benefits from a smaller noise intake compared to a wideband antenna setup due to a lower bandwidth. Compared to a tunable antenna with a similar bandwidth to that of the filtenna, a performance increase in the form of reduced system noise factor is seen. This reduced system noise factor comes from the elimination of the transmission line that tradi-

tionally connects the antenna and filter in the RF front end. With the noise benefits clear, the example filtenna used for this comparison is synthesized and simulated in the next sections.

Chapter 4

Filtenna Synthesis

As previously mentioned, the filtenna synthesis procedure closely follows that of a filter. Additional changes and parameters must be considered in order to fully integrate the antenna into the filtenna design. The goal of the filtenna synthesis procedure is to integrate the antenna as the last resonator in the design in such a way that the radiation and filtering capabilities are not greatly sacrificed. The end result of a successfully designed filtenna should be a single component that radiates in a similar fashion to the integrated antenna while also utilizing the antenna as a resonator in the filtering response.

4.1 Example Filtenna Design

The design of filtennas can be best shown through an example procedure. The design of this example filtenna starts with a standard filter synthesis. This involves calculating the g-coefficients of the filter based on the filter order and architecture. In this instance, the filtenna is based on a second-order 2% fractional bandwidth Butterworth bandpass filter with the g-coefficients seen in Table 1. These g-coefficients are used to calculate the inter-resonator couplings and external quality factors that are necessary to achieve the desired response.

Second-Order Butterworth Coefficients			
$\mathbf{g_0}$	$\mathbf{g_1}$	$\mathbf{g_2}$	$\mathbf{g_3}$
1	1.4142	1.4142	1

Table 4.1: Table of the lowpass filter prototype coefficients for a second-order Butterworth filter.

The inter-resonator coupling for an ideal second-order Butterworth bandpass filter with a fractional bandwidth of 2% is calculated using the process outlined earlier and results in a coupling value of $k_{12} = 0.014142$. The external quality factors necessary were also calculated using the filter synthesis approach and found to be $Q_{ext1} = Q_{ext2} = 70.71$. The inter-resonator coupling between the resonators in this design is achieved through the use of an inductive iris that is commonly used to couple between cavities. The external coupling for the filter side is achieved through a coplanar waveguide (CPW) feed with arcing wings to produce the required coupling as seen in Fig. 4.2. The width and length of the wings of the CPW feed can be adjusted to change the external quality factor and therefore the coupling into the first resonator [27]. The external coupling on the antenna side is more complicated and is discussed in more detail in the next section.

The inter-resonator coupling between the first and second resonators in the design is achieved through an inductive iris. The amount of coupling this iris provides can be adjusted by changing the size of the iris. A wider iris leads to stronger coupling and a thinner iris leads to weaker coupling. This method of inter-resonator coupling was chosen as it can be easily realized to connect the two cavity-based resonators in this design.

Another important detail in filter synthesis is the choice and design of the resonators. For this design, an evanescent-mode cavity is used as the first resonator and was designed using the methods found in [27] and [28]. This cavity has excellent

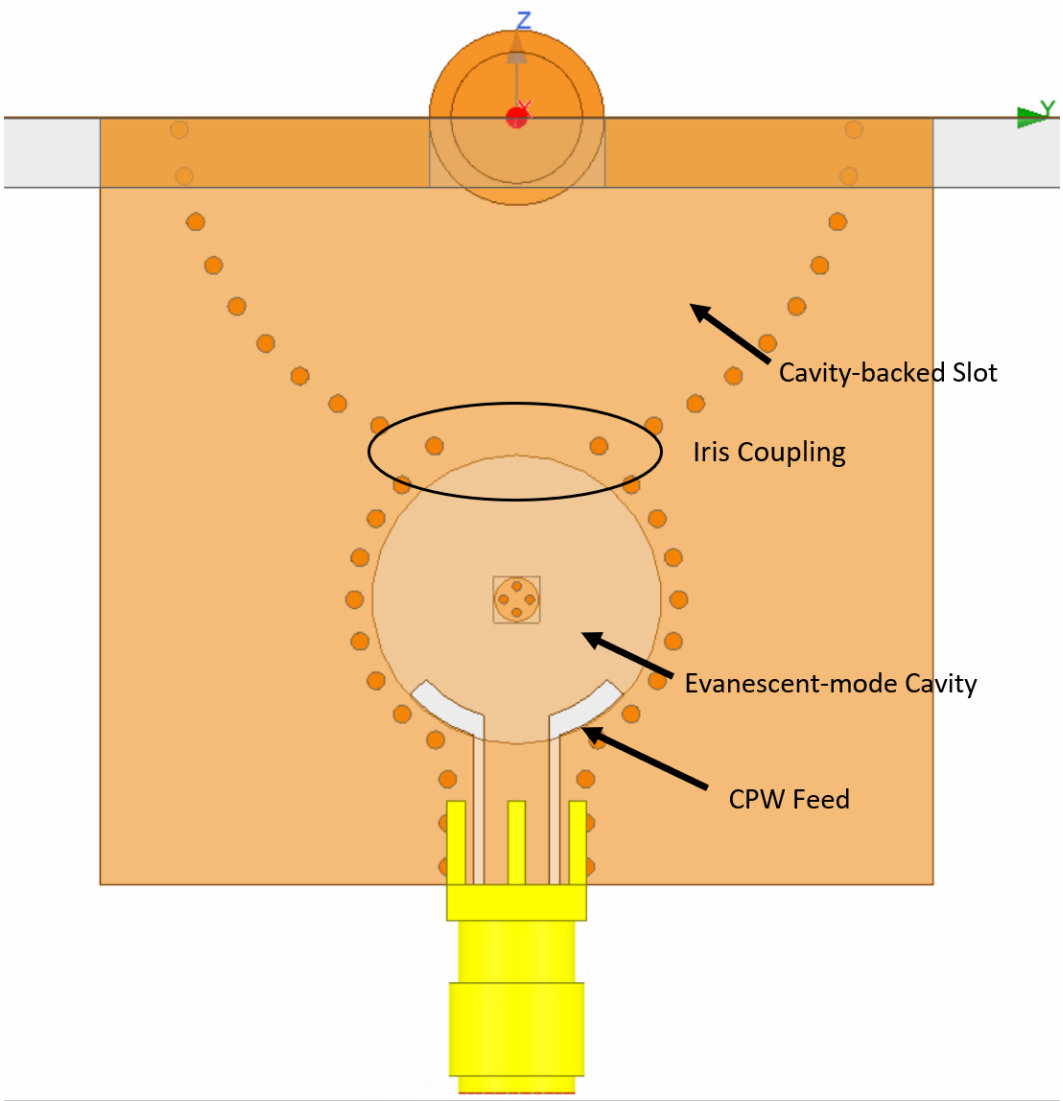

Figure 4.1: Overall view of the filtenna with different sections highlighted.

performance with low insertion loss and high power-handling while still remaining tunable. The cavity is tuned by changing the air gap above the center vias or post. Increasing the size of the air gap increases the distance between the center post and the top copper sheet, decreasing the amount of capacitance loading the cavity, and thereby increasing its operating frequency. Decreasing the air gap increases the capacitance, further loading the cavity and decreasing its operating frequency. The

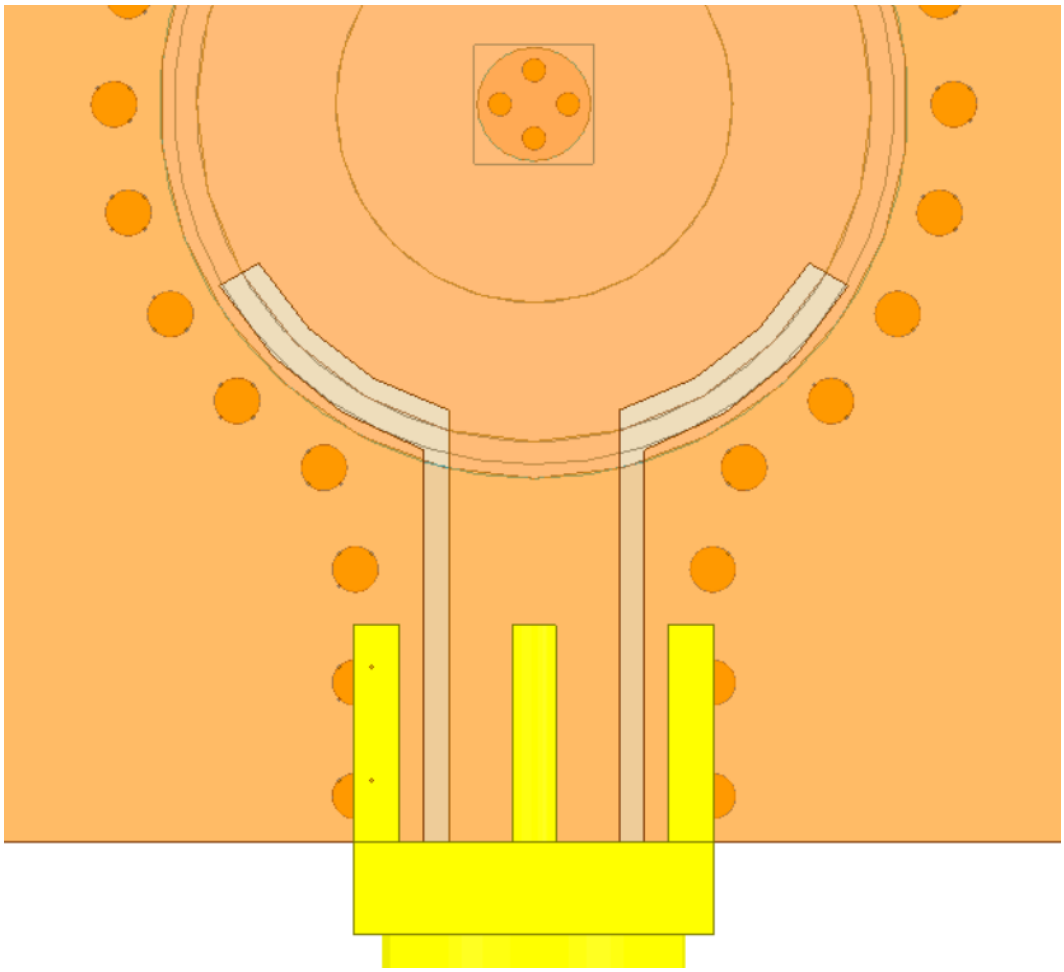

Figure 4.2: CPW feed for the filter side of the filtenna.

air gap size is controlled by a piezoelectric actuator device from Piezo Systems Inc. (PN: T216-A4NO-273X) which can be biased with a DC voltage from -180 volts to 180 volts and can be tuned a full octave from 2 GHz to 4 GHz.

The second resonator in the design is where the synthesis changes from a purely filter-oriented approach to a filtenna-oriented approach. Instead of another standard filter resonator, an antenna is used. The cavity-backed slot antenna used in this design acts as both a resonator for the filter and as a radiating element. The important parameter of the antenna external quality factor will be investigated in the next section. The card insert portion of the filtenna design encompasses most of the

overall filtenna excluding the ground plane for the cavity-backed slot and is seen in Fig. 4.1. The card insert for this design was chosen to be made from a 125 mil thick board of Rogers TMM3. This means that the slot aperture has a width of 125 mil and the cavity-backing and evanescent-mode cavity which are built into the TMM3 card insert have a height of 125 mil.

4.1.1 Cavity-Backed Slot

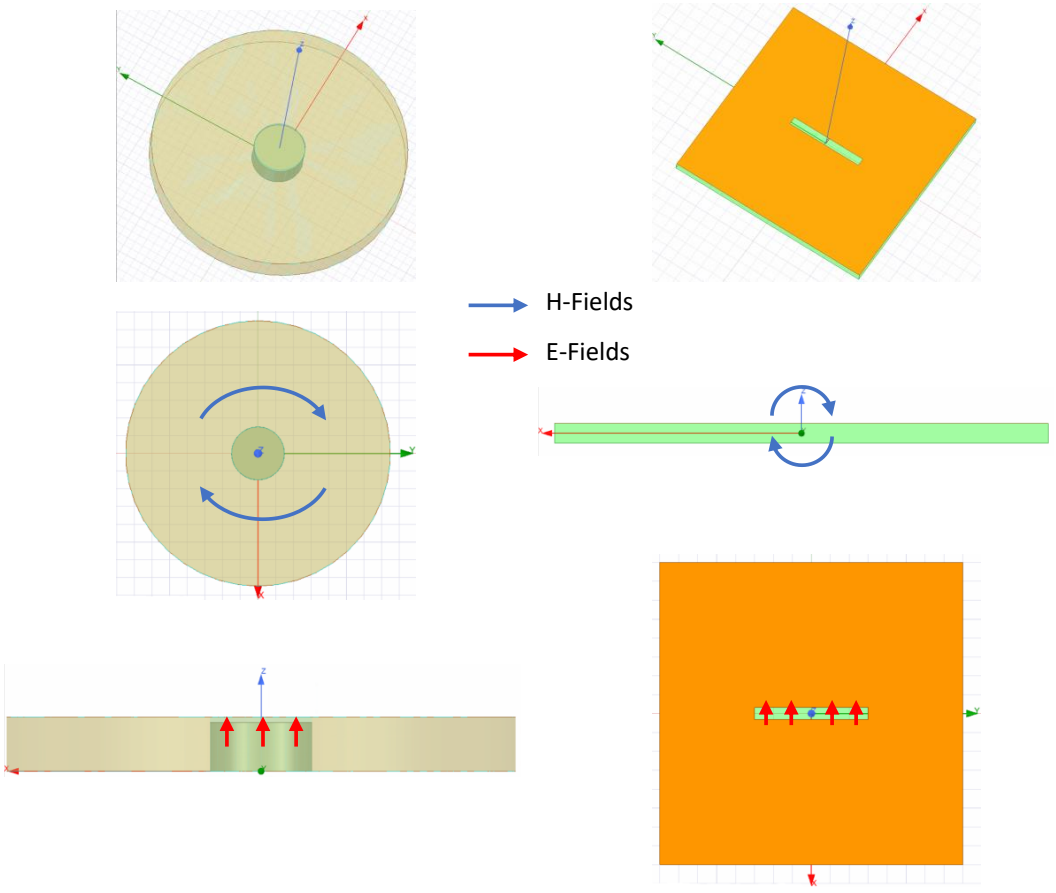

Figure 4.3: Field distributions for the HMSIW cavity and the slot antenna.

The antenna used in this design is a half-mode substrate integrated waveguide

(HMSIW) cavity-backed slot antenna. The idea for using this cavity for the slot antenna comes from the field distribution. The field distribution of the cavity in this form is extremely similar to that of a standard slot antenna as can be seen in Fig. 4.3. Since the field distributions of both the cavity and the slot are extremely similar they can be easily integrated into a cavity-backed slot.

The cavity-backing for the cavity-backed slot design is based on a tunable evanescent-mode cavity resonator. This cavity was designed similarly to the other evanescent-mode cavity resonator in the filtenna but was cut in half to produce a half-mode substrate integrated waveguide. In addition to cutting the cavity in half, an open boundary condition must be enforced along the now open face of the cavity to ensure the half-modes behave as expected [29]. This open boundary condition can be easily achieved through the use of a slot antenna which can span the open face of the cavity to complete the cavity-backed slot.

The cavity backing allows for a radiation pattern with a higher front-to-back ratio and allows for easier coupling from the evanescent-mode cavity through an inductive iris. The cavity-backed slot antenna is tuned through a capacitive-loading post in a similar fashion to the evanescent-mode cavity. The post is controlled by a NewScale Technologies M3-L linear actuator that moves the post back and forth. The closer the post gets to the other side of the slot antenna, the higher the capacitive loading is and the lower the operating frequency becomes.

The aperture of the slot has a length 38 mm while the backing cavity has a diameter of 30 mm. This mismatch is to allow for easier fabrication. The added slot aperture length allows for a card insert version of the evanescent-mode cavity to be fabricated which is detailed more thoroughly in Chapter 6. The vias of the cavity-backing near the slot aperture ensures that any fields that might extend past the cavity-backing along the slot aperture are shorted and thereby eliminated.

Cavity-Backed Slot Investigations

Some aspects of the cavity-backed slot were investigated to ensure that the behavior was satisfactory. These investigations included changing the size of the slot aperture without changing the size of the cavity-backing as well some investigations into the resonating behavior of the cavity-backed slot.

The gain and frequency of the filtenna are not at all impacted by shortening the slot aperture until the slot aperture is shorter than the diameter of the backing cavity at 30 mm. At that point, the frequency starts shifting upwards and the gain is decreased slightly. This behavior is subtle at first, but as the slot aperture is made even shorter the effects grow. This can be at least partially explained due to the heavy loading of the cavity-backed slot due to the frequency reconfigurability. The tuning post at the center of the cavity-backed slot applies capacitive loading that concentrates the fields near this central point. This means that changes near the edge of the slot aperture will have a significantly smaller effect on the overall behavior of the cavity-backed slot than changes near the center.

Eigenmode simulations of the cavity-backed slot in HFSS appear to show that there exists only one resonance for that entire structure. There does not seem to be a separate resonance for the slot and the cavity backing. The behavior of the cavity-backed slot is consistent with that of a half-mode cavity that is bounded by a perfect H field instead a slot aperture.

4.2 Frequency Reconfigurable S-band Filtenna

When both of the resonators in the design are correctly tuned to the specified frequency, the gain response of the filtenna approximates a second-order Butterworth bandpass response. It should be noted that the fractional bandwidth of the

design changes based upon where the center frequency is tuned to. This is due to the inability to tune the external couplings and the inter-resonator couplings on the fly with this design. As a result, the filtenna has a fractional bandwidth of approximately 2% at its center frequency of 3 GHz, with a lower fractional bandwidth below that frequency and a larger fractional bandwidth above that frequency.

4.3 Conclusions

An example second-order tunable filtenna was presented that makes use of an evanescent-mode cavity and a cavity-backed slot antenna. This filtenna is able to tune a full octave across the S-band from 2 GHz to 4 GHz with a 2% fractional bandwidth at 3 GHz. Additional investigations into the cavity-backed slot antenna were conducted to ascertain whether it was truly operating as a cavity-backed slot or instead as a leaky waveguide. From the investigations it seems that the cavity-backed slot antenna is indeed operating as intended. With the example design laid out a closer look at the external coupling of the cavity-backed slot, and therefore that of the filtenna design, is in order.

Chapter 5

Filtenna External Coupling

While a filtenna can follow the analytic filter synthesis relatively closely, there are some changes that are necessary to produce and incorporate the radiating structure. Instead of the traditional last resonator, an antenna compatible with the rest of the structure must be designed. While there are many different antenna geometries capable of being integrated into filtennas, there remains the problem of matching the external quality factor of the filter side to the external quality factor of the antenna. There is plenty of literature in the antenna world concerning the total quality factor of an antenna, however there is a lack of information regarding the external quality factor of antenna. This is due to the external quality factor being a mostly filter-oriented characteristic and thus an analogue between filter theory and antenna theory must be made.

5.1 External Quality Factor of the General Antenna

The quality factor of a resonator can be defined as the ratio between the power stored in the resonator and the power lost in one cycle. In standard filter theory, a lossless resonator will have an infinite quality factor as there is no way for the stored power in the resonator to be dissipated. The typical equation that is used to

find the quality factor of a resonator is,

$$\frac{1}{Q_L} = \frac{1}{Q_U} + \frac{1}{Q_{ext}}, \tag{5.1}$$

where Q_L is the loaded quality factor of the resonator, Q_U is the unloaded quality factor of the resonator, and Q_{ext} is the external quality factor. This equation can still be used for an antenna, but the understanding of what each quality factor means changes slightly as antennas radiate power away as well as dissipate power through ohmic and dielectric losses. In the case of lossless antennas, the unloaded quality factor of the antenna will tend towards infinity due to the lack of loss, thereby eliminating the $\frac{1}{Q_U}$ term in 5.1. The only term left that could characterize the antenna's quality factor then would be Q_{ext}. Therefore, the external quality factor of an antenna is simply the quality factor from the power radiated and is equivalent to finding the quality factor of the lossless antenna [30]. The quality factor of the lossless antenna is also known as the radiation quality factor of the antenna making the external quality factor of an antenna its radiation quality factor. The radiation quality factor of the antenna, and therefore the external quality factor that is necessary for use in filtenna design, can be obtained from the overall quality factor of a lossy antenna using the equation outlined in [31],

$$Q_{rad} = \frac{Q}{\eta}, \tag{5.2}$$

where Q is the overall quality factor of the lossy antenna and η is the radiation efficiency of the same antenna.

Another shortcoming of the current filtenna literature is the reliance of filter-oriented methods for extracting the external quality factor of an antenna. These

methods include extracting the external quality factor of the antenna through the use of an equivalent circuit representation as well as through other common filter extraction methods using the return loss of the resonator [20],[32]. Since the radiation quality factor, or lossless quality factor, of the antenna has been shown to be the antenna equivalent of the external quality factor, the vast general antenna literature can be leveraged to find faster and simpler ways of finding the external quality factor. A rather straightforward way to obtain the external quality factor of an antenna would be to find the lossless antenna's input impedance. There is a plethora of different methods that can be used to find the quality factor of a lossless antenna as shown in the antenna literature, but this work will primarily be using the input impedance. As far as the author knows, this method has not been used before in the filtenna literature to extract the external quality factor of the antenna. Other methods of obtaining the quality factor of an antenna has been extensively studied in the antenna literature and as such many different ways can be applied for use in finding the external quality factor of the general antenna [33].

Equipped with the input impedance of the antenna, the quality factor of the lossless antenna can be found using the equation,

$$Q(\omega) = \frac{\omega}{2R_0(\omega)}\sqrt{\left[R_0'(\omega)\right]^2 + \left[X_0'(\omega) + \frac{|X_0|}{\omega}\right]^2}, \tag{5.3}$$

where $R_0(\omega)$ is the untuned resistance of the antenna, $R_0'(\omega)$ is the derivative of the resistance of the antenna with respect to frequency, and $X_0'(\omega)$ is the derivative of the reactance of the antenna with respect to the frequency [34].

Since the input impedance of an antenna is a well studied topic there are a plethora of approaches to obtaining the required information to characterize the external quality factor of an antenna for use in filtenna design. It should be noted

that any approach to obtain the antenna's lossless radiation quality factor will suffice to find the external quality factor.

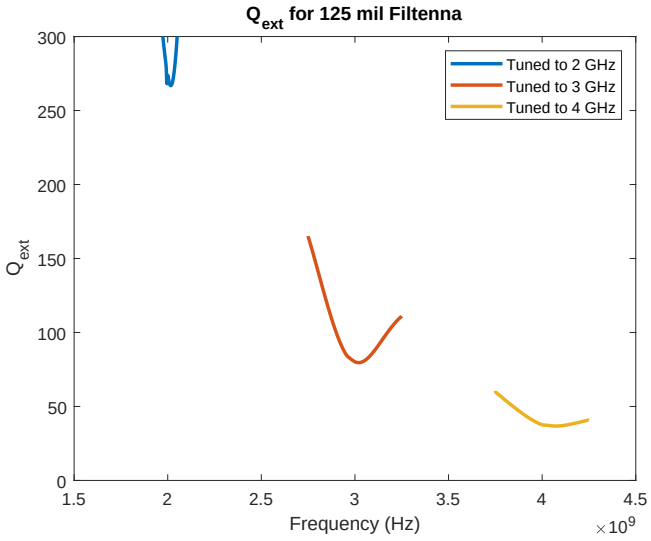

Figure 5.1: External quality factor for the 125 mil filtenna.

5.2 External Quality Factor of Example Cavity-backed Slot

The external quality factor of the cavity-backed slot from the example filtenna across frequency is shown in Fig. 5.1. As can be seen, the radiation quality factor spikes near the lower edge of the frequency band of interest. This results in a large external quality factor mismatch between the filter port side and the antenna side. This mismatch combined with the inability to tune the rest of the couplings in the filtenna leads to a decrease in bandwidth and eventual pole splitting at the lower frequencies. At the higher edge of the frequency band of interest, the external quality factor is lower than the ideal value of 70.71 for a 2% bandwidth filtenna. This in addition to the inability to tune the other couplings in the design results in a fractional bandwidth that is larger than ideal. This response of the filtenna across

frequency can be seen in Fig. 5.2. The filtenna performs the best at the initial design frequency of 3 GHz with slight reductions in gain as the filtenna approaches its tuning limits. The reduction seen near the lower frequencies can be attributed to a decrease in both radiation efficiency and mismatch efficiency compared to the 3 GHz tuning. The loss of radiation efficiency is primarily due to the heavy loading necessary on the cavity-backed slot to achieve the lower frequencies. The loss in mismatch efficiency, which is also the primary reason for the very slight reduction in realized gain at the higher frequencies, can be attributed to the lack of tunability of the external couplings of the filtenna design.

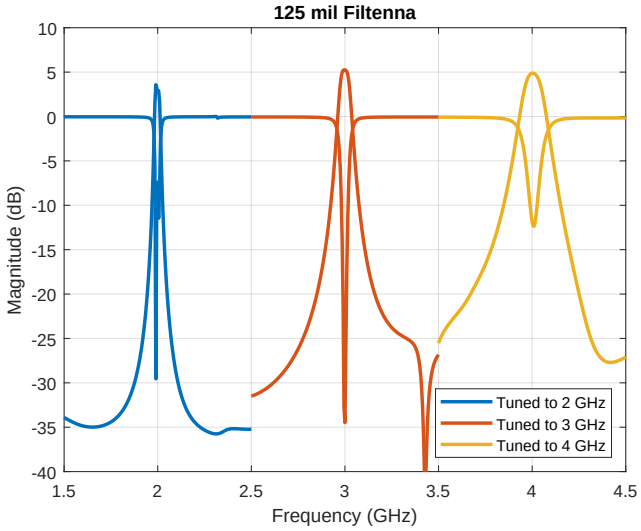

Figure 5.2: Gain response for the 125 mil filtenna.

The radiation patterns for the filtenna can be seen in Fig. 5.3a and Fig. 5.3b. These radiation patterns closely resemble those of a standard cavity-backed slot complete with an increased unidirectional radiation due to the cavity backing. It should be noted that the cross polarization radiation in Fig. 5.3a is too small to easily represent in the figure.

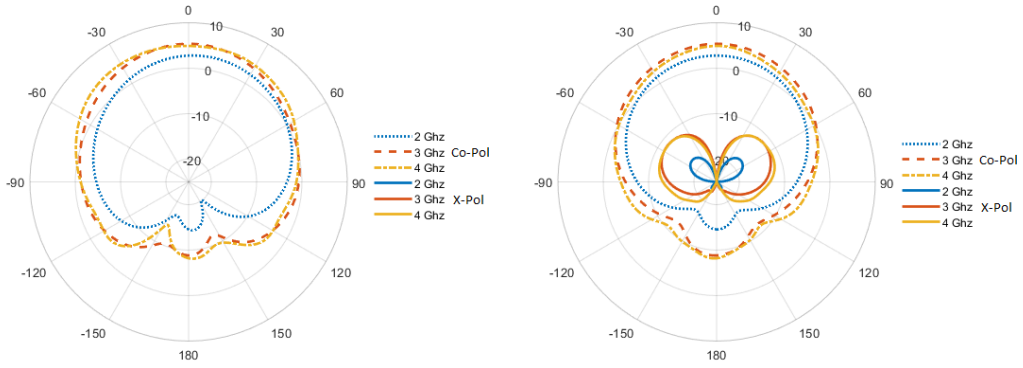

(a) $\phi = 0°$ (b) $\phi = 90°$

Figure 5.3: Radiation Pattern for the 125 mil slot width filtenna.

5.2.1 Cavity-Backed Slot Width Variations

While the base design utilizes a card insert with a height of 125 mil and therefore a slot aperture with that same width, this parameter can be varied. Using the input impedance equation to find the lossless radiation quality factor, and therefore the external quality factor of the cavity-backed slot, shows that a wider slot leads to a lower overall external quality factor across frequency while a thinner slot leads to a higher external quality factor. As with coupling apertures in filter theory, a lower external quality factor results in a stronger coupling and vice versa. In this case, a wider slot and card insert increases the area of the aperture and allows for a stronger coupling to free space.

The filtenna design was altered to work with a slot width and card insert height of 60 mil instead of the previous 125 mil. This thinner aperture should result in a higher radiation quality factor and a lower coupling to free space. This is indeed the result as can be seen in Fig. 5.4. The external quality factor values for the 60 mil slot width version of the cavity-backed slot is substantially larger than its 125 mil slot width counterpart.

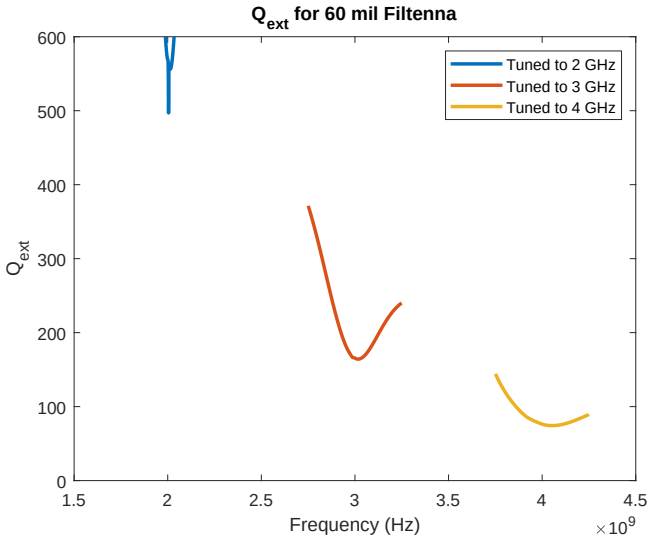

Figure 5.4: External quality factor for the 60 mil filtenna.

The external coupling on the filter side was then adjusted by reducing the width and length of the CPW feed wings to better match this higher external coupling factor and produce a lower external coupling. Time domain tuning was then used to retune the resonators and inter-resonator coupling to incorporate the new external quality factors at 3 GHz. Once the new parameters were found for the thinner insert filtenna at 3 GHz, only the resonators were retuned to work at 2 GHz and 4 GHz using the tunable piezoelectric actuator and linear actuator in this design. This produced the responses shown in Fig. 5.5 with performance comparable to the 125 mil filtenna. The bandwidth of the filtenna decreased with the increase in external quality factor and decrease in external coupling as would be expected. It should be noted that the radiation efficiency of the thinner filtenna is decreased compared to the normal width filtenna especially at the band edge of 2 GHz as can be seen in Fig. 5.7. The combination of the heavy loading of the cavity-backed slot and the thinner slot aperture width greatly decreased the radiation efficiency.

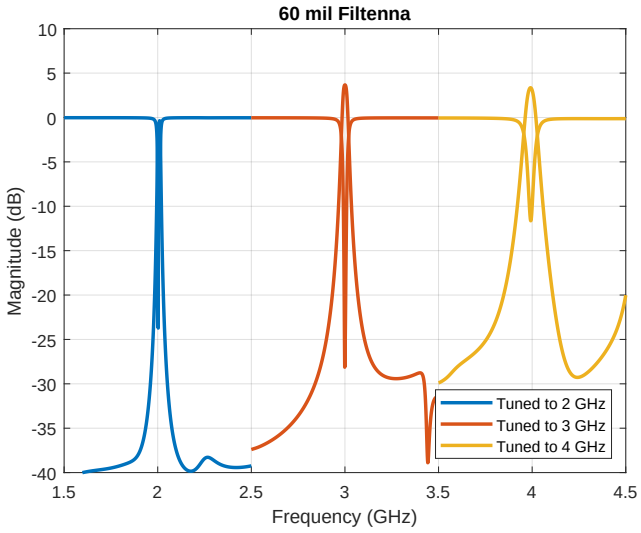

Figure 5.5: Gain and S_{11} for the 60 mil filtenna.

Table 5.1: External quality factor of the cavity-backed slot at different slot aperture widths.

	60 mil Aperture	125 mil Aperture	200 mil Aperture
2 GHz	564	266.8	171.9
3 GHz	166.7	79.9	50.1
4 GHz	76.1	37.5	23.5

The radiation patterns of the 60 mil slot width variation of the filtenna, shown in Fig. 5.6a and Fig. 5.6a, are consistent with the 125 mil version and cavity-backed slots in general. The loss in radiation efficiency especially at the lower frequencies did decrease the co-polarized gain quite a bit, while the cross-polarization stayed relatively the same.

The slot aperture and card insert were both then thickened to 200 mil producing a lower external quality factor as seen in Fig. 5.8. Similarly to the external quality factor relationships in the 60 mil and 125 mil versions, the external quality factor

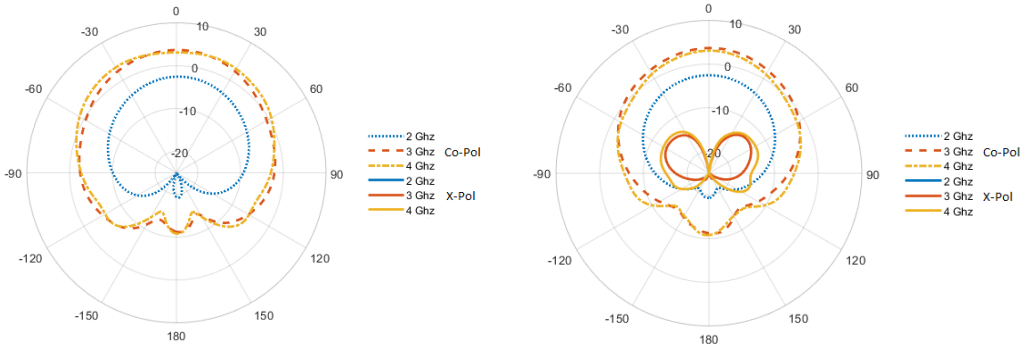

(a) $\phi = 0°$ (b) $\phi = 90°$

Figure 5.6: Radiation Pattern for the 60 mil slot width filtenna.

near the lower frequencies changes rapidly across frequency. However, the change across the different slot width variations shows that the thicker slot widths produce external quality factors that are less sensitive to frequency changes.

Again, time domain tuning was used to tune the resonators and inter-resonator coupling to better match the new external quality factor at 3 GHz. The additional thickness made tuning the filtenna to lower frequencies slightly easier as the gap sizes necessary to tune down to 2 GHz were not as small. The opposite result was seen with the thicker slot aperture compared to the thinner slot aperture with the bandwidth increasing due to the decrease in the external quality factor and subsequent retuning of the filtenna.

The resulting external quality factors for all of the different slot width cavity-backed slots is summarized in Table 5.1.

It should be noted that any discontinuities or extremely sharp changes in external quality factor seen in the figures are a result of sharp changes inherent in the input impedance. As the step size of the input impedance used in calculating the external quality factor decreases, the discontinuities disappear and the figures approach the true external quality factors.

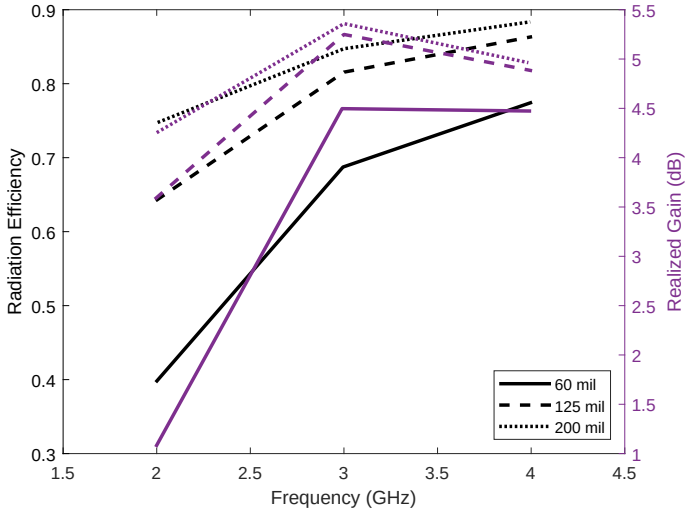

Figure 5.7: Radiation efficiency and realized gain of the filtennas with varying card insert and slot aperture widths. Black lines represent the filtenna's radiation efficiency at the particular frequency and purple lines represent the filtenna's realized gain at the particular frequency.

In summary, increasing the card insert width and slot aperture width of the cavity-backed slot results in a decrease in external quality factor of the antenna and an increase in the external coupling to free space while the opposite is true when the width is decreased. In fact, this relationship between the slot width and the resulting external quality factor of the antenna is simply inversely proportional. If the external quality factor is normalized by the slot width, as seen in Fig. 5.11, the cavity-backed slots of varied widths all behave the same across frequency. This indicates that the relationship between the slot width and the resulting external quality factor is relatively simple with the frequency of operation of the cavity-backed slot playing a more complex role.

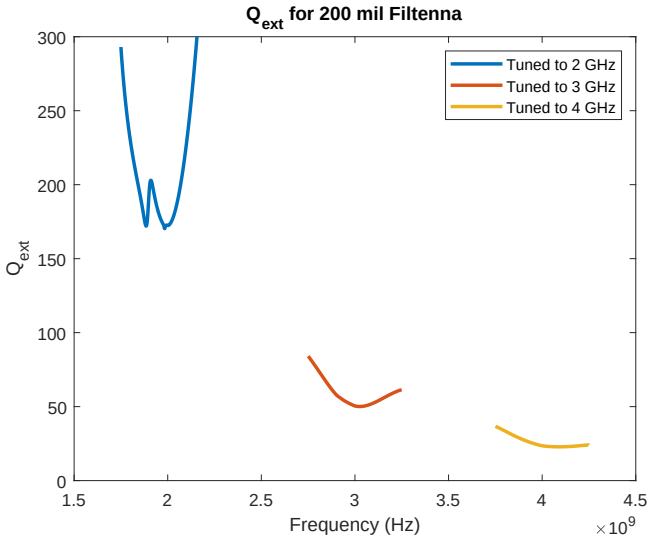

Figure 5.8: External quality factor for the 200 mil filtenna.

5.2.2 Cavity-Backed Slot Aperture Length

The same result as was seen in the width variations can be seen when the length of the slot is changed. An increase in length decreases the external quality factor and a decrease in length increases the external quality factor. In essence, a larger overall area of the cavity-backed slot aperture leads to a increase in external coupling and a smaller area leads to an decrease in external coupling. It should be noted that the slot aperture in this design extends past the cavity-backing. This was done in order to streamline the fabrication process and allow for the card insert portion which contains the cavity backing as well as the evanescent-mode cavity and the rest of the filtenna to be more easily integrated with the ground plane of the slot. The extension of the aperture, however, has little to no effect on the overall behaviour of the cavity-backed slot as the extended portion is shorted with a via from the cavity backing. This can be seen in Fig. 5.12 with the via shorting across the slot aperture. This short means that there are little to no fields that extend past this point. This

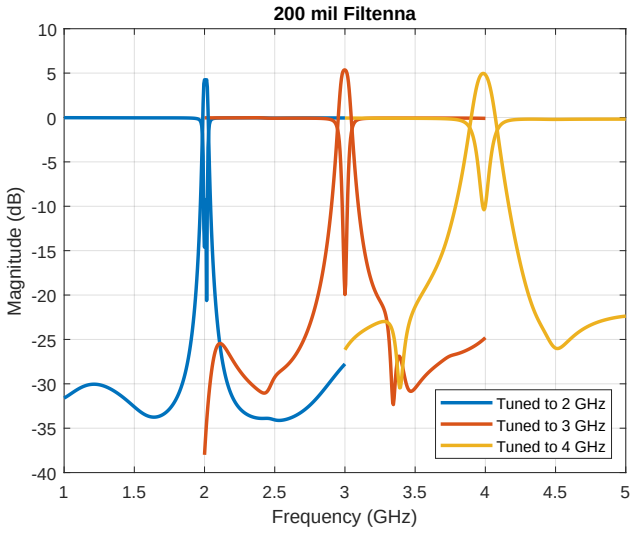

Figure 5.9: Gain and S_{11} for the 200 mil filtenna.

results in the aperture being the same size as the cavity backing, electromagnetically speaking.

While the operating frequency does change with a change in slot length as in a traditional slot or cavity-backed slot antenna, this phenomenon is heavily impacted by the tuning of the filtenna. When the filtenna is tuned to 4 GHz and the capacitive post has the least impact, a change in slot length changes the operating frequency similarly to a non-tunable slot antenna. However, when the slot is heavily loaded in the center by the capacitive post, a change in slot length impacts the operating frequency very little. This is due to the majority of the fields in the cavity-backed slot antenna being constrained to the very center where the loading is taking place. Since this change in aperture length of the cavity-backed slot does affect both the external quality factor and frequency of operation at the same time, this is not an ideal method for manipulating the external quality factor for use in filtenna design. The slot aperture width seems to be a better method, only majorly impacting the

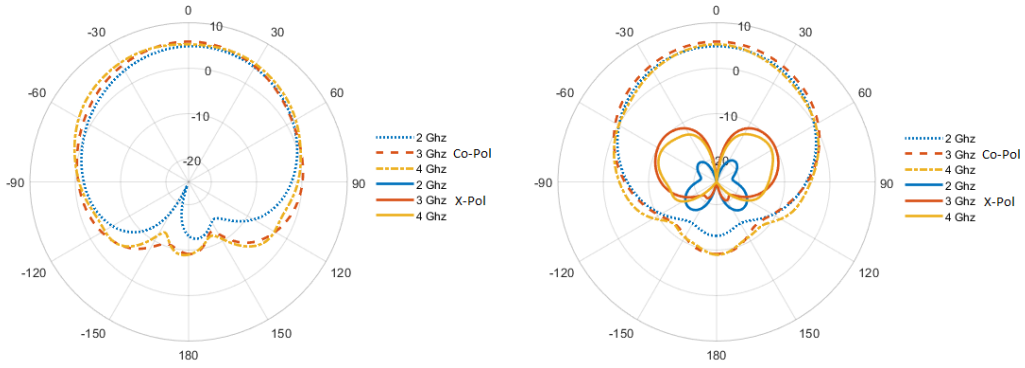

(a) $\phi = 0°$ (b) $\phi = 90°$

Figure 5.10: Radiation Pattern for the 200 mil slot width filtenna.

radiation efficiency of the cavity-backed slot if the aperture is made very thin.

5.3 Conclusions

The relationship between an antenna's general quality factor, which is heavily discussed in the antenna literature, and its external quality factor has been shown. By approaching an antenna as a simple resonator it have been shown that the external quality factor of an antenna is simply its lossless quality factor also known as its radiation quality factor in the antenna literature. As far as the author knows, this link has never been definitively stated in the filtenna literature. This more rigorous understanding of the nature of an antenna's external quality factor allows for the utilization of methods from the antenna literature to extract an antenna's quality factor. While there are many methods defined in the antenna literature to extract this parameter, such as through current densities or through the stored and far fields, a method based on the input impedance of the antenna was chosen. This input impedance method is straightforward to implement to extract the quality factor of an antenna through various simulations. Now that the external quality factor of an

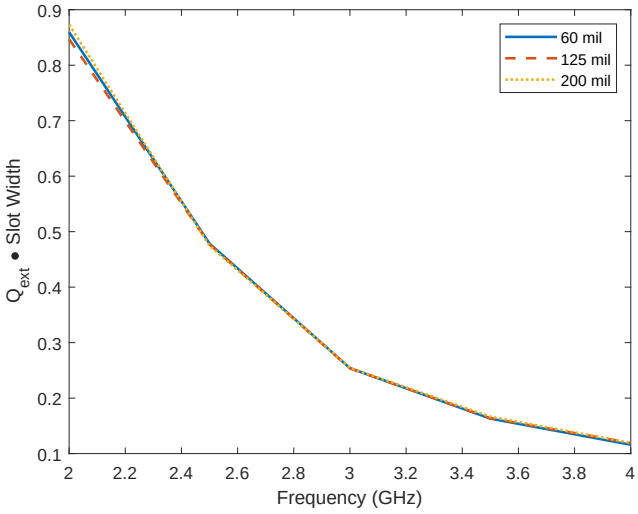

Figure 5.11: Normalized external quality factor for the slot width variations of the cavity-backed slot across frequency.

antenna can be easily extracted, this parameter can be used to advance a proposed filtenna design.

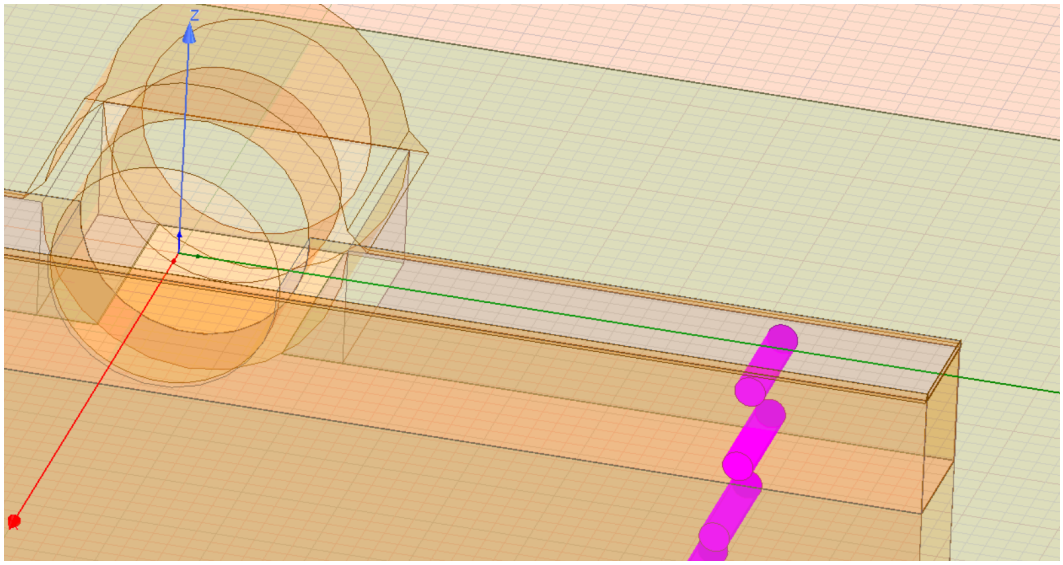

Figure 5.12: Vias shorting any additional fields on the slot past the cavity-backing.

Chapter 6

Fabrication and Results

The new external quality factor extraction method for filtenna design that has been presented will now be applied in practice. A filtenna design is simulated and subsequently fabricated as described below.

6.1 Filtenna Simulation

A filtenna was designed according to the synthesis process outlined earlier. The first resonator of the second-order Butterworth bandpass filter was designed as an evanescent-mode cavity resonator. The second resonator of the design was replaced by a cavity-backed slot antenna. The design was implemented in HFSS to simulate the expected results.

6.1.1 Filtenna Tuning

Time domain tuning was used to fine-tune the filtenna once the design parameters were set. The focus was on tuning the evanescent-mode cavity resonator using a piezoelectric actuator and tuning the cavity-backed slot using a capacitive tuning post controlled by a linear actuator. Time domain tuning is a method of tuning that works well for higher order filters as well as lower order filters. The step-by-step

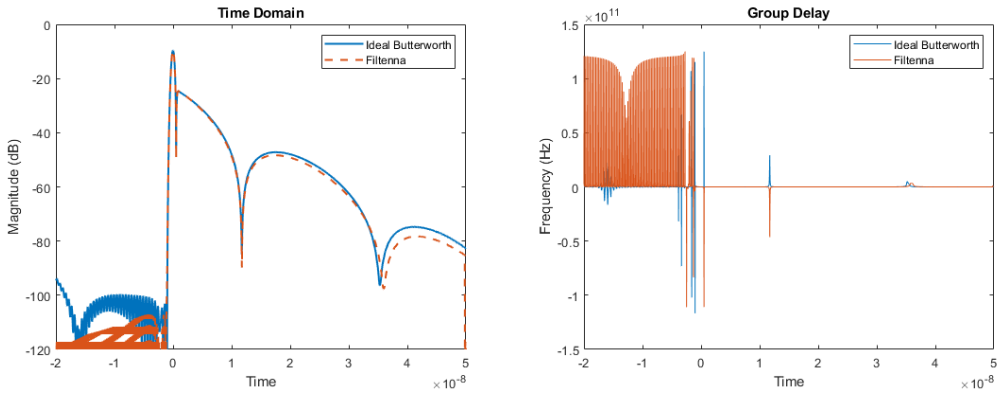

(a) Time domain. (b) Group delay of time domain.

Figure 6.1: Time domain representation of a second-order Butterworth bandpass filtenna and the ideal time domain response for a second-order Butterworth bandpass filter.

approach helps streamline the tuning approach providing the starting point of the tuning is somewhat close already. If the resonators in the design are extremely far from being correctly tuned for a given frequency of operation, it can be difficult to know whether to tune that resonator up or down in frequency.

The time domain representation for a filter, or in this case a filtenna, usually looks similar to that seen in Fig. 6.1a. A series of humps with nulls represent the tunings of the couplings and the resonators. The humps represent the couplings of the filter or filtenna and the nulls represent the tuning of the resonators in the design. It should be noted that in the example shown and in most time domain representations there will be more humps and nulls than there are couplings and resonators in the actual structure. You must start with the left most hump as in the external coupling into the structure and then work your way tuning left to right. In addition, errors from previous couplings and resonators will compound into later structures meaning that fine tuning early resonators and especially couplings can lead to more accurate tuning in later parts of the filter or filtenna [27].

In the given example, there are two resonators with two external couplings (one

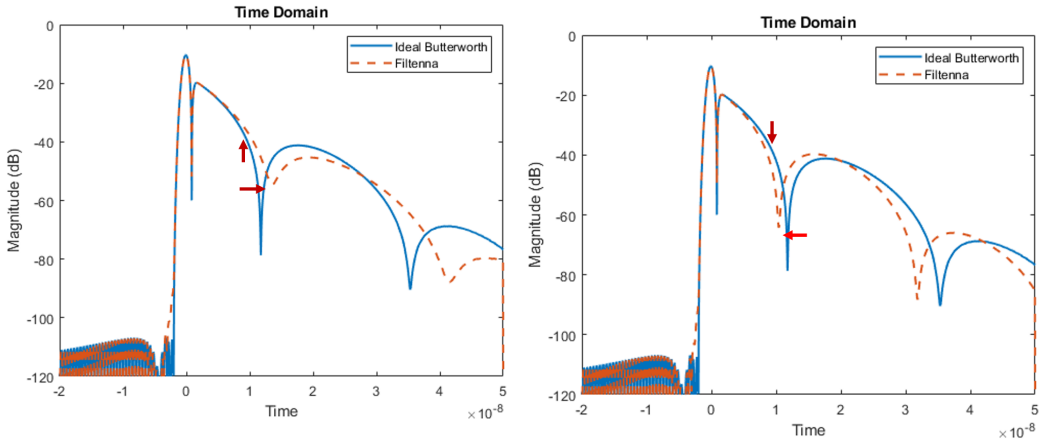

(a) Time domain of an undercoupled response.

(b) Time domain of an overcoupled response.

Figure 6.2: Time domain representation of a second-order Butterworth bandpass filtenna with mistuned inter-resonator coupling.

into the structure and one out) and one inter-resonator coupling. Therefore anything after the third hump in the time domain representation can safely be ignored. The time domain representation can be found by taking the inverse discrete Fourier transform (IDFT) of the windowed, linear, complex S_{11} of the structure.

Any nulls or humps seen before a time of zero, especially those that have a significantly smaller magnitude and are closer together in time as seen in Fig. 6.1a are a result of ringing. Various different windowing functions can be used to try to mitigate this issue. These of course can be ignored as they are just noisy artifacts. The same can be seen in Fig. 6.1b with the artifacts instead having a very large magnitude. In addition, the response of the filtenna under test or the ideal response might need to be slightly shifted in time in order for the two responses to line up correctly. This can also be done more accurately with more precise deembedding in simulation or in measurement.

To start tuning, an ideal filter should be synthesized as a good standard to tune to. This ideal time domain response will be used as a template while tuning the

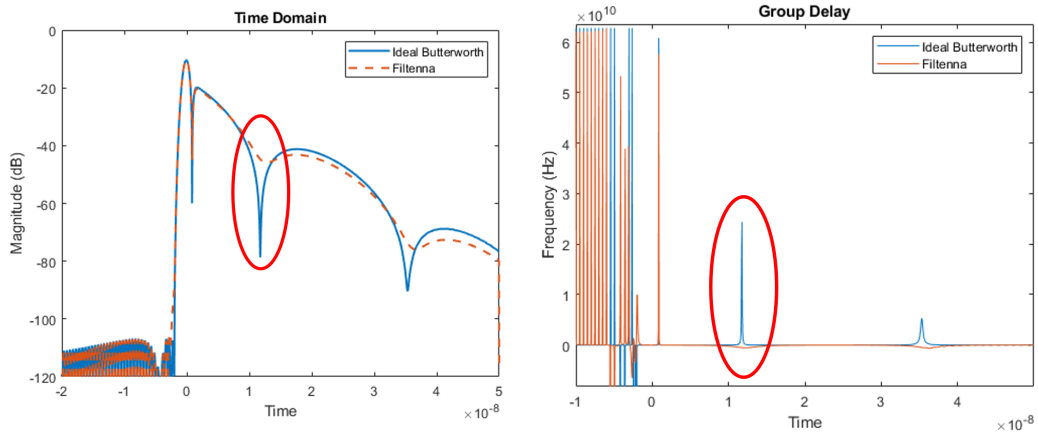

(a) Time domain of mistuned filtenna.

(b) Group delay of mistuned filtenna.

Figure 6.3: Time domain representation of a second-order Butterworth bandpass filtenna with the circled resonator mistuned below the ideal response.

desired design. Tuning the couplings of the design is usually very straightforward by looking at just the time domain representation. A hump that is pushed further forward in time and higher in magnitude than the ideal response as seen in Fig. 6.2a signifies that the coupling is undercoupled. A hump that is pushed back in time and has a lower magnitude than the ideal as seen in Fig. 6.2b signifies that the coupling is overcoupled. The same behavior is seen in any coupling regardless if it is an external coupling or an inter-resonator coupling.

Tuning resonators in the time domain is slightly more complicated and relies on using the group delay of the time domain. This can be found with the equation:

$$\tau = \frac{\partial \arg(T(t))}{\partial t}, \tag{6.1}$$

where $T(t)$ is the time domain representation of the structure [27]. The time domain representation of a mistuned resonator appears the same regardless if the resonator is tuned too high or too low in frequency compared to the ideal tuning. Both sub-optimal tunings will appear as shallow dips, as seen in Fig. 6.3a, instead of deep

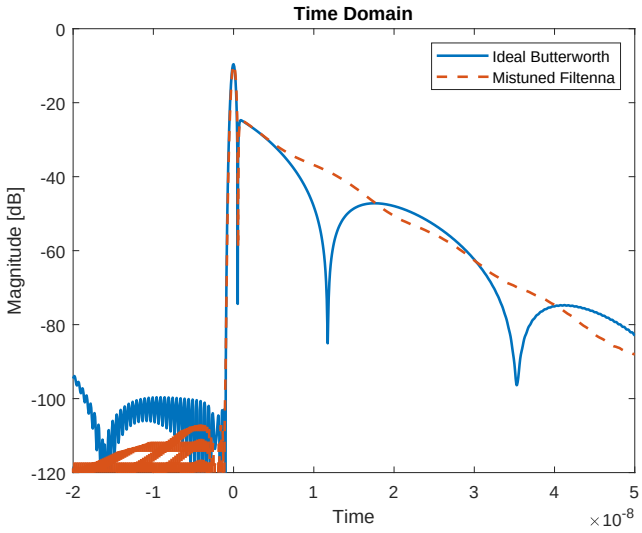

Figure 6.4: Time domain of the filtenna at 3 GHz with a severely mistuned cavity-backed slot resonator.

nulls with no indication as to which way to tune the resonator. If the resonator is severely mistuned there will be no dip or null at all resulting in a straight line that makes it appear as if there is no resonator at all. An example of the phenomenon can be seen in Fig. 6.4.

By referencing the timing of the nulls in the normal time domain representation, the spikes in the group delay of the time domain that correspond to the resonators can be found. These spikes will change in magnitude as the tuning of the resonator changes. If the spike corresponding to the resonator under investigation is negative and smaller in magnitude than the ideal response as seen in Fig. 6.3b, then the resonator is below the desired frequency. If the spike is positive and smaller in magnitude than the ideal response as seen in Fig. 6.5b, then the resonator is above the desired frequency. If the resonator starts tuned below the ideal frequency as in 6.3b and it is tuned up in frequency, the magnitude of the spike start to increase. This magnitude continues to increase as the resonator is tuned higher in frequency until

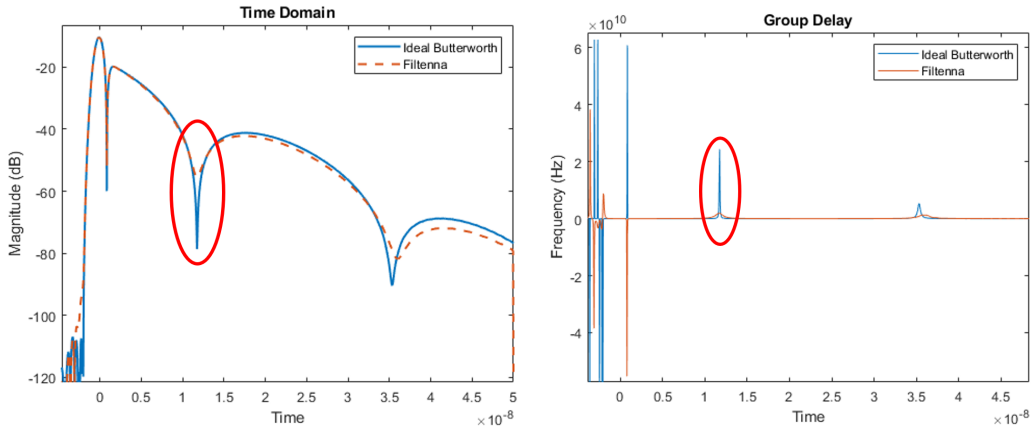

(a) Time domain of mistuned filtenna.

(b) Group delay of mistuned filtenna.

Figure 6.5: Time domain representation of a second-order Butterworth bandpass filtenna with the circled resonator mistuned above the ideal response.

the spike turns from negative to positive. As the resonator's frequency continues to be increased, the magnitude of the spike starts to decrease as the desired frequency is overshot and the resonator becomes tuned too high in frequency.

It should be noted that as the magnitude of the spike representing the resonator increases it becomes more sensitive. As such, even if the spike is not exactly at the same magnitude as the ideal response, as long as it has a fairly large magnitude then that resonator can be considered well tuned. When the magnitude of the resonator is very large even a small change in tuning can result in overshooting the ideal response and flipping the sign of the spike. As long as the magnitude remains large and the S_{11} response of the filtenna looks good, then the sign of the spike corresponding to the resonator to be tuned does not matter too much. This is why the rather well tuned filtenna seen in Fig. 6.1a and Fig. 6.1a has resonator spikes that do not have the same sign as the ideal response.

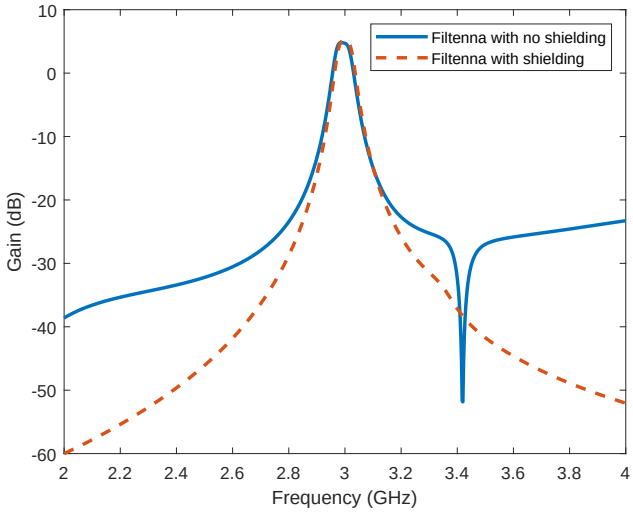

Figure 6.6: Comparison of the filtenna with and without shielding the CPW feed.

6.1.2 Realized Gain Null

From the simulation of the realized gain across frequency a deep null was found at approximately 3.43 GHz. Further analysis showed that the radiation efficiency and the match were not the cause of this null as they remained relatively consistent. In addition, tuning the filtenna to the frequency of the null did not show any impact in performance with the correct response being seen.

The ground plane of the slot antenna portion of the filtenna was then simulated to be infinite. This change restored the expected response and the null in the realized gain disappeared. This narrowed down the source of the null to be from the underside of the slot, potentially being caused by some errant field interaction. The offending component was found to be the CPW feed where some field leakage affected the realized gain over frequency. A small shielding box made of copper was simulated over the feed to stop any fields leaking from the feed and the null was resolved.

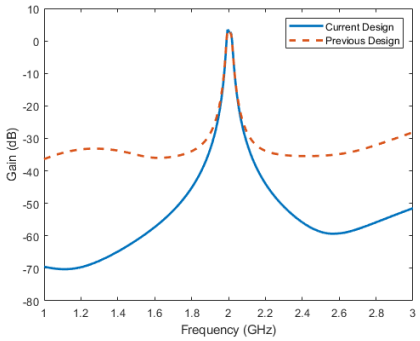

(a) Filtenna tuned to 2 GHz.

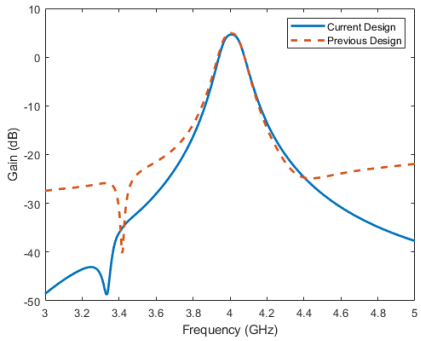

(b) Filtenna tuned to 4 GHz.

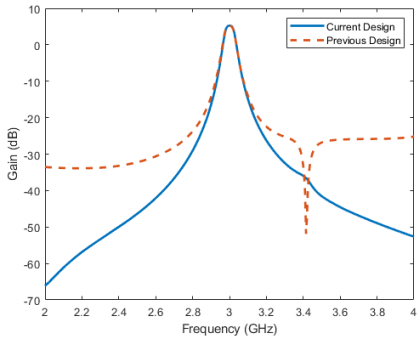

(c) Filtenna tuned to 3 GHz.

Figure 6.7: Comparison between the current filtenna design and the previous filtenna design.

In addition, shielding the CPW field to negate the effects of the leaking fields improved the out-of-band rejection of the filtenna by a considerable margin as seen in Fig. 6.6. This extra rejection was used in the noise comparison in Ch. 3, but was not included in the fabricated model as presented. Extra shielding can always be added to the fabricated model in the future to improve the out-of-band rejection. As the fabricated model does not have this shielding, the simulated version that it is compared to and seen in this and the previous section does not either. Additional testing of the fabricated version of the filtenna is warranted and planned to see if the same benefits seen in the simulated version of the filtenna with the shielding can be realized in the fabricated version.

6.1.3 New Design Simulation Results

The new design of the filtenna which used the new external quality factor method to easily extract a more accurate external quality factor for the filtenna design was compared to the previous filtenna design from [27]. The changes made include a modification of the CPW feed to better match the newly extracted external quality factor and the addition of the previously discussed CPW feed shield. The results in Fig. 6.7 show that the slight change in external quality factor does not produce a larger change in the overall results between the two filtennas. The addition of the CPW feed shield, however, leads to a significant increase in out-of-band rejection at all the filtenna tunings. While the new extraction method does not produce wildly different results compared to older methods in the filtenna literature, it does provide a more streamlined approach resulting in an easier overall design process.

6.2 Filtenna Fabrication

In order to verify the simulations and theory discussed previously in this work, a second-order Butterworth filtenna was fabricated with a 125 mil thick card insert. The filtenna used the same design with a cavity-backed slot and evanescent-mode cavity resonator as was discussed. The piezoelectric actuator that was used to tune the evanescent-mode cavity resonator worked very well once the slightly tricky process of fabrication was completed. The linear actuator that was used to control the tuning post to tune the cavity-backed slot was not an ideal method for a very fine granularity of tuning at lower frequencies, but the fabricated filtenna was still able to provide good performance throughout the entire S-band from 2 GHz to 4 GHz.

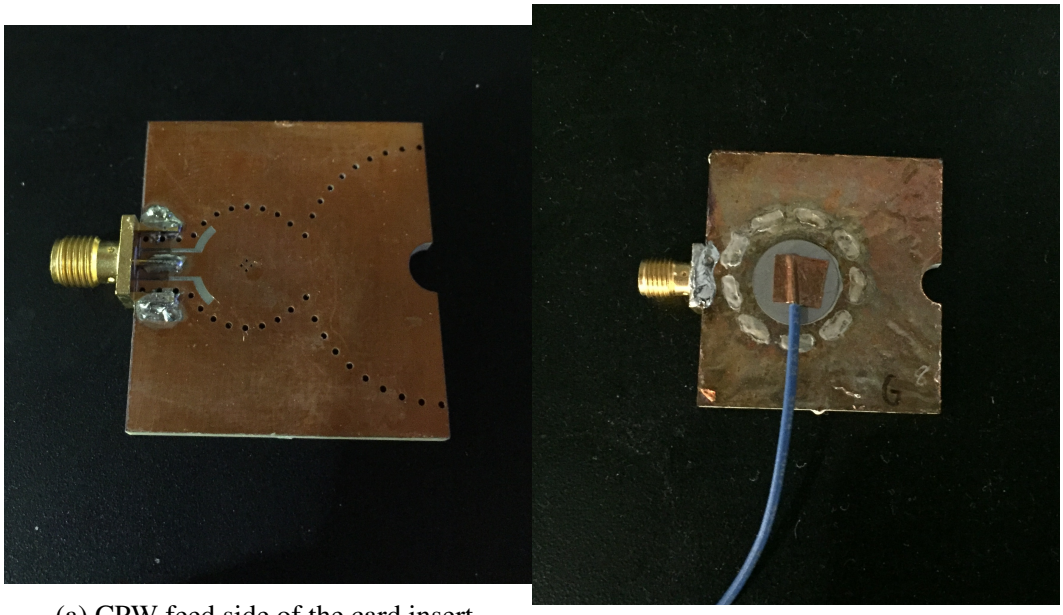

(a) CPW feed side of the card insert.

(b) Group delay of mistuned filtenna.

Figure 6.8: Piezoelectric actuator side of the card insert.

6.2.1 Card Insert Fabrication

The card insert which includes the cavity-backing for the slot antenna portion of the filtenna and the evanescent-mode cavity for the filter portion of the filtenna was constructed starting with a 125 mil thick board of Rogers TMM3 substrate. Vias holes were drilled into the board using an LPKF ProtoMat S104 mill and then copper-plated through an electroless and electroplating process to create the cavities and the center post for the evanescent-mode cavity. Then, a CPW feed was laser-etched onto the board using an LPKF ProtoLaser U4 as a means for an SMA connector to couple into the first cavity. On the opposite side of the card insert, a thin layer of adhesive was laminated onto the board followed by a 1 mil thick sheet of copper. Care was taken to ensure there was an adequate air gap above the first cavity to allow for proper tuning of the evanescent-mode cavity which would be achieved by pushing and pulling the copper sheet layer via a biased piezoelectric actuator.

This involved milling a hole in the adhesive layer just above the evanescent-mode cavity. Once the copper sheet was laminated onto the board, the lack of the adhesive layer over the cavity itself created a small air gap. Holes were drilled through the copper sheet and adhesive layers and then filled in with LPKF ProConduct to ensure an electrical connection from the top layer of copper of the substrate to the copper sheet layer. LPKF ProConduct is a conductive material that is typically used to plate via through-holes without chemical or electroplating and thus allows a solid electrical connection from the top copper sheet to the copper layer of the TMM3 board. A piezoelectric actuator was then applied to the copper sheet directly over the air gap and evanescent-mode cavity using silver epoxy. A small wire was attached to the piezoelectric actuator in order to apply the voltage necessary to tune the cavity. The other lead for the DC bias voltage can be connected or clipped on directly to the copper of the rest of the card insert. An SMA connector was then soldered onto the insert before it was tested for proper tuning behavior. A completed card insert example can be seen in Fig. 6.8a with the CPW feed side shown. On the opposite side of the card seen in Fig. 6.8b is the extra copper sheet layer with the piezoelectric actuator affixed with the silver epoxy and the attached wire for voltage control.

6.2.2 Slot Ground Plane Fabrication

The ground plane for the cavity-backed slot was constructed using a six inch by six inch 125 mil thick Rogers TMM3 substrate. First the slot outline as well as an additional outline to fit in the post and post guide was cutout. The board was then copper plated using an electroless plating process followed by electroplating process to apply approximately 15 μm of copper to the board. The point of this

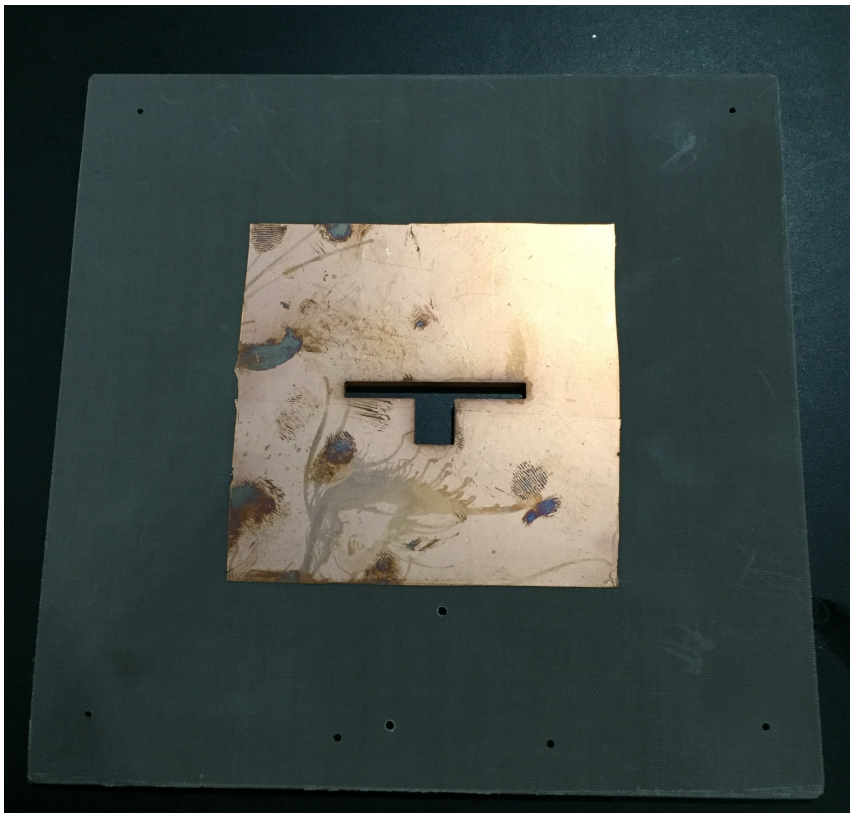

Figure 6.9: Filtenna ground plane for the 125 mil filtenna.

step was to plate the inside edge of the cutout where the post guide and card insert would sit. The side wall of the cutout would serve as a conducting plate to complete the capacitor made with the tuning post. The closer the tuning post gets to the side wall of the cutout, the larger the capacitance and the lower the frequency the filtenna would tune to. Once the plating was complete, the most of the copper on the top and bottom face of the ground plane was etched away using a photolithography process. The remaining ground plane was 80 mm by 80 mm on the top and 45 mm by 20 mm on the bottom. The 80 mm by 80 mm ground plane on the top ensured a good directivity of approximately 6 dB. Care was taken to ensure that the etching fluid could not reach the inside walls of the cutout so that they would remain plated. This was done by covering the copper that needed to remain after the etching process

with Kapton tape to protect the copper from the etching fluid. This was done on the front of the board to leave the correct amount of copper for the ground plane. The back side of the board also needed Kapton tape applied to it so that the etching fluid could not enter the cutout and the copper on the inside edge of cutout would be preserved. This resulted in some copper having to remain on the back side of the board. A completed ground plane example can be seen in Fig. 6.9.

Figure 6.10: Back of the completed 125 mil filtenna.

6.2.3 Filtenna Integration

Once the two boards were completed and the card insert was tested for proper tuning, the final integration of the two could begin. The card insert was anchored into place using solder, ensuring both structural integrity as well as a solid electrical connection. Another prototype was tested using a silver epoxy as the anchoring medium, but the structural integrity was not ideal. The silver epoxy was not strong enough to support the card insert in an acceptable manner so that line of fabrication was abandoned. The card insert soldered into the ground plane can be seen in Fig. 6.10.

With the card insert firmly fixed into place, the post guide and tuning post could be situated. The two components were lined up and affixed to the ground plane using copper tape as solder was not easily adhering to the surface of the copper post guide. A small 3D-printed part was fastened to the tuning post to allow for a thin rod to be attached. The rod was attached to another 3D-printed part that was screwed to the linear actuator. This whole assembly, seen in Fig. 6.11, allowed for the linear actuator to push and pull the tuning post to a few micrometers of precision.

6.3 Filtenna Measurements

The fabricated filtenna was measured using a few methods to verify that the design worked as expected. This included measurements in the time domain to verify that the filtenna was able to be fine tuned as desired for optimal performance.

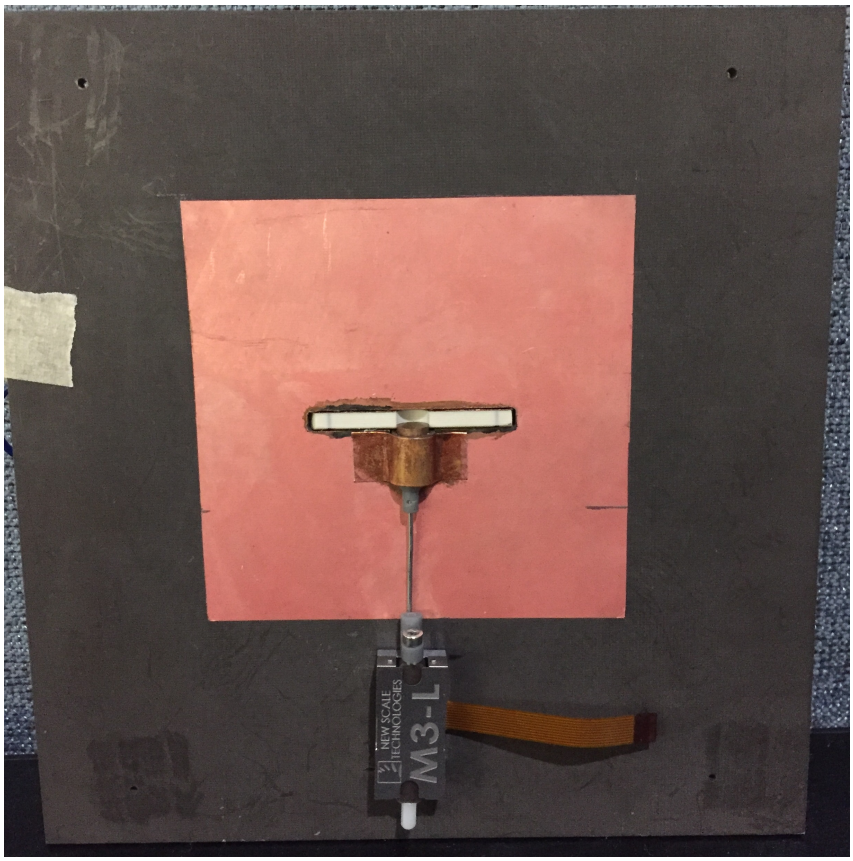

Figure 6.11: Front of the completed 125 mil filtenna.

6.3.1 Card Insert Measurements

Once the card insert was fabricated it needed to be tested to ensure it could properly tune across the entire S-band. A DC power supply was used to bias the piezoelectric actuator for tuning, with one lead connected to the piezoelectric actuator via a wire and the other clipped onto the copper layers of the card insert. The use of this power supply necessitated a DC-block when using the network analyzer for measurements. The card insert's S_{11} was measured using the network analyzer and good tuning from 2 GHz to 4 GHz was achieved. Once the card insert was verified to tune across the entirety of S-band, it was integrated into the full filtenna as outline earlier.

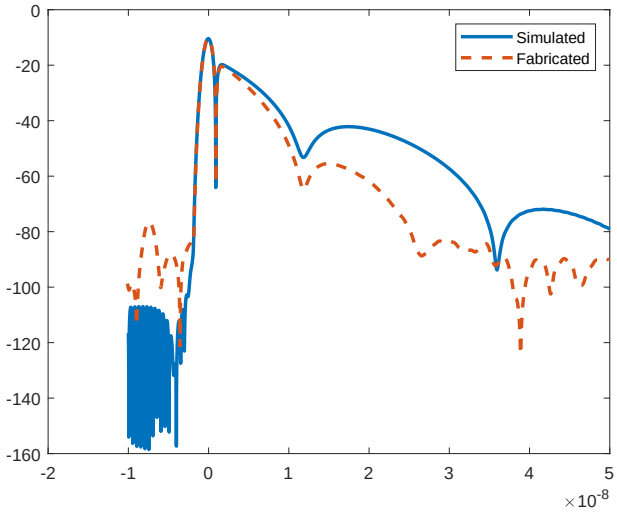

Figure 6.12: Comparison of the time domain between the fabricated and simulated filtenna at 3 GHz.

6.3.2 Time Domain Measurements

An important part in insuring that the filtenna was well-tuned during measurements was the use of time-domain tuning discussed earlier. The Vector Network Analyzer (VNA) that was used included a time domain package that allowed for real-time time-domain viewing. Some trouble was encountered due to the noise floor of the VNA sometimes covering up and corrupting some of the nulls that are important and inherent in the time-domain view. While decreasing the IF bandwidth of the VNA did not have noticeable effects on the noise floor in the time-domain, increasing the number of points in each sweep did allow for better null identification. More points in the sweep meant that the nulls of the time-domain representation were better presented and finer adjustments could be made. A larger number of points, however, does increase the amount of time taken for each sweep of the VNA which can result in significant time delays between filtenna adjustments and

the resulting measurements. This can be alleviated by increasing the IF bandwidth which does not seem to majorly impact the resolution in the time-domain nor does it majorly impact the noise floor in the time-domain.

The time domain measurements for the fabricated filtenna at 3 GHz can be seen in Fig. 6.12 with the ideal simulated time domain for comparison. This time domain measurement lines up quite well with the simulated response. The input external coupling is as simulated, as is the tuning of the evanescent-mode cavity resonator. The inter-resonator coupling seems to be as expected at 3 GHz with some added loss compared to the simulated verison. The output external coupling of the fabricated version does deviate compared to the simulated version. This can be explained by the environment in which the time domain results were measure. The measurments took place on a workbench near large amounts of metal. Since the output external coupling of a filtenna is due to the radiation of the structure, the nearby metal will affect the measured output external coupling seen in all the time domain results. The time domain measurements for the fabricated filtenna at 2 GHz and 2.5 GHz can be seen in Fig. 6.13a and Fig. 6.13b, respectively, with the ideal simulated time domain for comparison. The time domain measurements for the fabricated filtenna at 3.5 GHz and 4 GHz can be seen in Fig. 6.14a and Fig. 6.14b, respectively, with the ideal simulated time domain for comparison. While the time domain for the filtenna tuned to 3 GHz looked as expected compared to the simulated version, the other time domain responses are off to some extent. While the resonator tunings and other couplings in the design seem to match simulations relatively well, these time domain responses indicate that the inter-resonator coupling of the fabricated filtenna is more sensitive to frequency than the simulated filtenna. This is almost certainly due to fabrication issues. The two vias in the filtenna design that control the inductive iris width that controls the inter-resonator coupling may

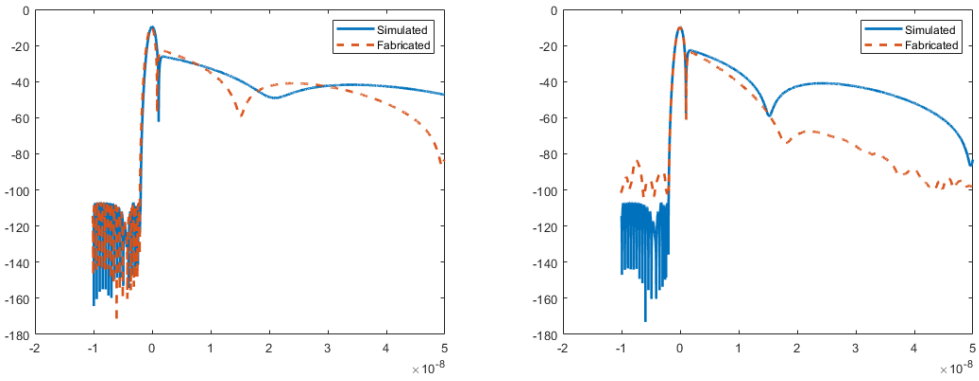

(a) Time domain at 2 GHz.

(b) Time domain at 2.5 GHz.

Figure 6.13: Comparison of the time domain between fabricated and simulated filtenna.

have not been properly copper-plated. This could have introduced the extra frequency dependency in the inter-resonator coupling of the fabricated filtenna which would explain the discrepancies between the simulated and fabricated filtenna time domain measurements.

6.3.3 Filtenna Tuning Measurements

The filtenna was successfully able to tune across the entire S-band from 2 GHz to 4 GHz with an acceptable S_{11}. The measurements require the tuning of the filtenna and therefore control over the piezoelectric actuator and the linear actuator in the design. During testing a DC power supply was used to control the piezoelectric actuator for the evanescent-mode cavity and a laptop was used to control the linear actuator for the cavity-backed slot portion of the filtenna. The measurement setup can be seen in Fig. 6.15.

The results compared to simulations can be seen in Fig. 6.16. The return loss for the 3 GHz, 3.5 GHz, and 4 GHz tunings are better than expected while the return loss for the 2 GHz and 2.5 GHz tunings is worse than expected. This can be mostly

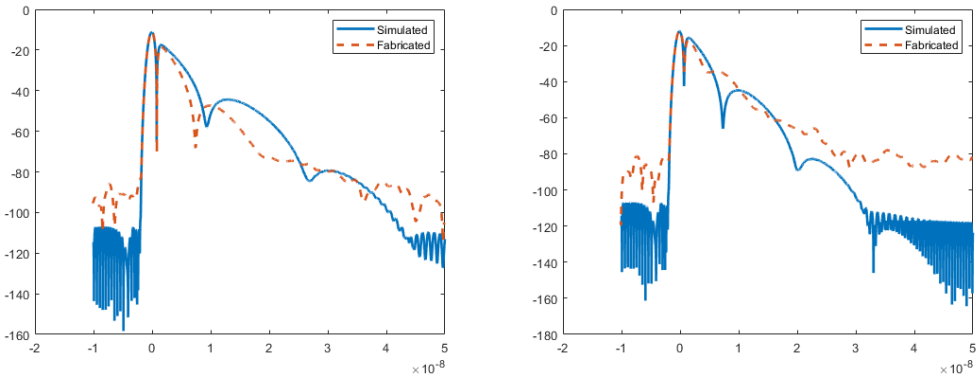

(a) Time domain at 3.5 GHz.

(b) Time domain at 4 GHz.

Figure 6.14: Comparison of the time domain between fabricated and simulated filtenna.

explained by the inter-resonator coupling issue due to fabrication that is discussed in the previous section.

The fabricated measurement at 2 GHz does leave something to be desired due to tuning sensitivity limitations. The primary factor in this is the linear actuator in charge of tuning the cavity-backed slot. While this tuning mechanism works admirably at higher frequencies, near the lower band edge of 2 GHz the linear actuator is not capable of small enough distance changes. The actuator is only capable of changes down to 0.5 μm, which is too large of a change to accurately tune at 2 GHz. Since the gap between the tuning post and the back wall of the cavity-backed slot is so small at the lower frequencies, a distance of 0.5 μm creates a relatively large change in capacitance that causes the tuning to overshoot the target of 2 GHz.

6.4 Conclusions

An example filtenna design was advanced and modified with the use of the new external quality factor extraction method. This design was subsequently fabricated

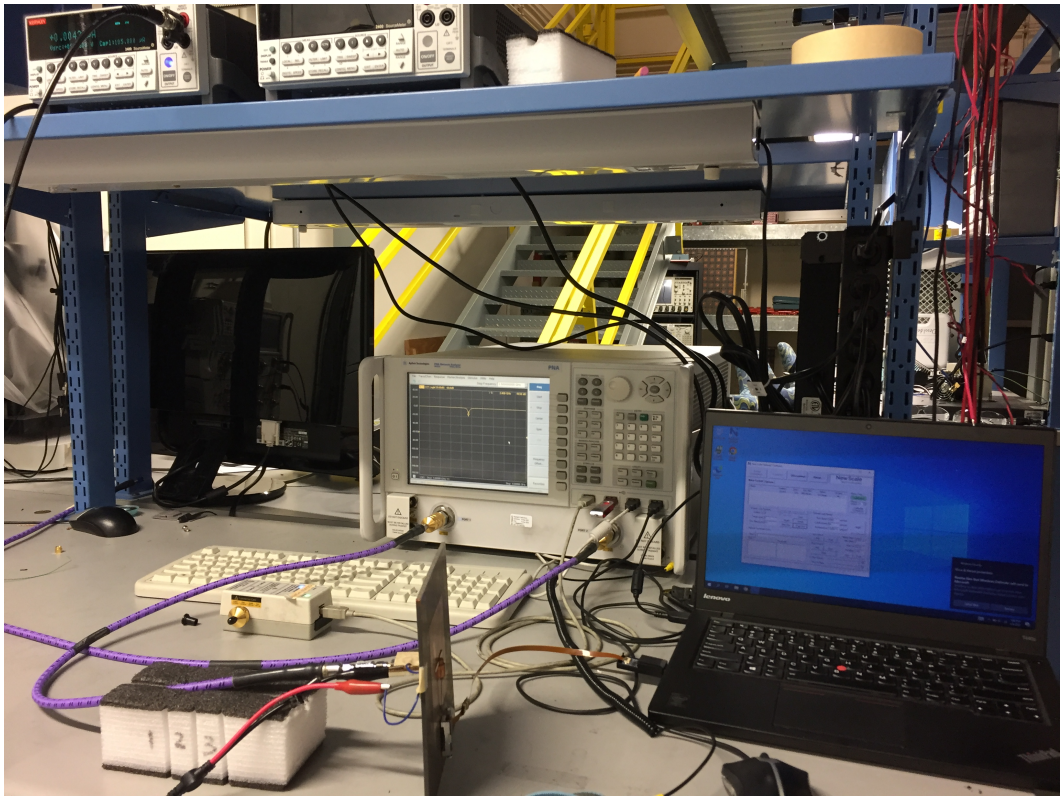

Figure 6.15: Measurement setup for the time domain and return loss of the filtenna.

and measured for validation. The fabricated filtenna matches the simulated version relatively well and tunes across the entire S-band from 2 GHz to 4 GHz. The time domain measurements of the fabricated filtenna point towards a small issue in fabrication affecting the inter-resonator coupling which negatively impacts the results at 2 GHz and 2.5 GHz. While this small fabrication error negatively impacts the filtenna at lower frequencies, the return loss of the filtenna is actually improved at 3 GHz and above. The overall results were satisfactory and the design has been validated.

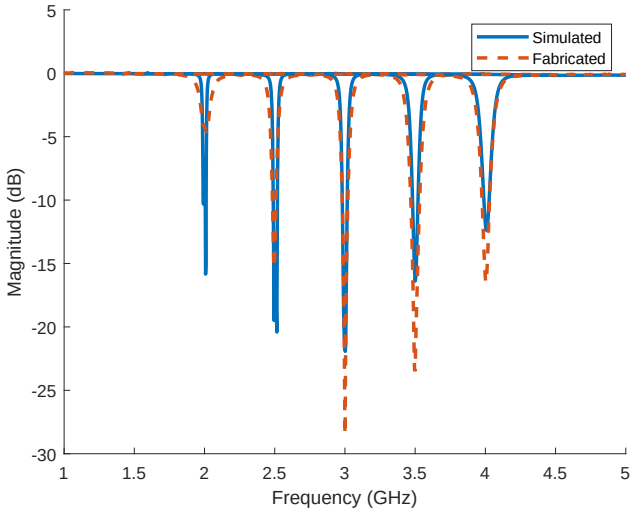

Figure 6.16: Comparison of the return loss between the fabricated and simulated filtenna across S band.

Chapter 7

Conclusion and Future Work

The benefits of filtennas in terms of the size, weight, and power consumption of the RF front end is clear. The reduction of the overall footprint of the RF front end due to combination of the antenna and filter into one component as well as the elimination of the transmission line that typically connects the two can be applied to many areas such as spaceborne applications, aircraft, and automotive radar. In addition to the SWaP benefits of the filtenna, this work has shown that a tunable filtenna provides an improved noise figure over traditional RF systems without sacrificing radiation or filtering characteristics.

As filtennas continue to gain more interest and use, a more defined method of synthesis and design is necessary. With the findings in this work on the external quality factor of antennas, their use in filtenna design can more easily be understood and applied.

The external quality factor for an antenna has been established in this work with a straightforward method to find this parameter. This parameter is incredibly important for the design and synthesis of filtennas which must use and incorporate the external quality factor of the antenna for optimal integration. There is no in depth discussion on the external quality factor of an antenna in the literature to the best knowledge of the author and as such the explanation and examples provided in

this work will be helpful for the design of future filtennas.

This work has also shown that the external quality factor of this cavity-backed slot can be manipulated by changing the size of the slot aperture in the design. These manipulations can be used to better match the ideal design parameters for a given filtenna and produce simulations and fabricated filtennas that better resemble ideal filter responses.

With the information and insights presented in this thesis which aid in the streamlined design of the general filtenna, filtennas should continue to grow in popularity.

7.1 Future Work

Filtennas show many benefits over traditional designs and present many opportunities for continued work in their area. Investigations into a few topics of interest for both the near and further future are planned.

7.1.1 Anechoic Chamber Measurements

Anechoic Chamber measurements to determine the realized gain of the fabricated filtenna as well as the effects of the unshielded CPW feed are planned. Due to the tunability of the filtenna these measurements are somewhat more complicated. In order to tune the evanescent-mode cavity resonator, DC power must be supplied to the piezoelectric actuator through a DC power supply during testing. This will involve a decently lengthy twisted pair that will have to be kept secure and stable as to not cause undue stress on the piezoelectric actuator. The linear actuator that controls the tuning for the cavity-backed slot must be connected to a laptop via a short ribbon cable. This can be quickly connected to tune the linear actuator and

then disconnected again. However, this may pose a problem when testing the lower frequencies where small changes in the state of the linear actuator can easily bring the filtenna out of tune. In the worst case scenario some sort of mount will have to be built to hold the laptop during testing so that the linear actuator can remain connected during testing.

7.1.2 Digital Phased Array

In the future, a multi-element digital phased array might prove to be an extremely useful application of filtennas. Many digital phased arrays must use a decent length of transmission line between the antenna and filter due to size and weight constraints. With many small elements needed to be a specified distance away from each other, there can be a lack of space to place filters for each element.

The greater out-of-band rejection this filtenna design has shown will also help alleviate problems associated with noise and interference for digital phased arrays. Since digital phased arrays primarily use a fan or spoiled beam to illuminate large scanning areas at time, the transmitted power, and therefore the reflected power, is spread out over larger areas leading to lower SINRs. A more sensitive system with larger amplifiers are commonly used which puts the system at more risk to interference. These systems can quickly become saturated with the combination of desired signals plus noise and interference which might lead to non-linearities or other problems.

References

[1] *United States frequency allocation chart*, Jan. 2016. [Online]. Available: https://www.ntia.doc.gov/page/2011/united-states-frequency-allocation-chart.

[2] A. M. Ali, H. Dinc, P. Bhoraskar, S. Bardsley, C. Dillon, M. McShea, J. P. Periathambi, and S. Puckett, "A 12-b 18-Gs/s RF sampling ADC with an integrated wideband track-and-hold amplifier and background calibration," *IEEE Journal of Solid-State Circuits*, vol. 55, no. 12, pp. 3210–3224, 2020.

[3] H. Jones, "The recent large reduction in space launch cost," 48th International Conference on Environmental Systems, 2018.

[4] M. Urcia and D. Banks, "Structurally integrated phased arrays," in *2011 Aerospace Conference*, IEEE, 2011, pp. 1–8.

[5] L. Baggen, S. Vaccaro, D. L. Del Rio, J. Padilla, and R. T. Sanchez, "A compact phased array for satcom applications," in *2013 IEEE International Symposium on Phased Array Systems and Technology*, IEEE, 2013, pp. 232–239.

[6] D. Rodrigo, J. Romeu, and L. Jofre, "Interference rejection using frequency and pattern reconfigurable antennas," in *Proceedings of the 2012 IEEE International Symposium on Antennas and Propagation*, IEEE, 2012, pp. 1–2.

[7] H. Rajagopalan, J. M. Kovitz, and Y. Rahmat-Samii, "MEMS reconfigurable optimized E-shaped patch antenna design for cognitive radio," *IEEE Transactions on Antennas and Propagation*, vol. 62, no. 3, pp. 1056–1064, 2013.

[8] A. Khidre, F. Yang, and A. Z. Elsherbeni, "A patch antenna with a varactor-loaded slot for reconfigurable dual-band operation," *IEEE Transactions on Antennas and Propagation*, vol. 63, no. 2, pp. 755–760, 2014.

[9] W. Ahmad and D. Budimir, "Reconfigurable UWB filtennas with sharp WLAN dual bandnotch," in *2015 European Microwave Conference (EuMC)*, IEEE, 2015, pp. 1228–1231.

[10] A. Mansoul, F. Ghanem, and M. Trabelsi, "A frequency reconfigurable antenna for high performance U-NII band radios," in *The 8th European Conference on Antennas and Propagation (EuCAP 2014)*, IEEE, 2014, pp. 1893–1895.

[11] A.-F. Sheta and S. F. Mahmoud, "A widely tunable compact patch antenna," *IEEE Antennas and Wireless Propagation Letters*, vol. 7, pp. 40–42, 2008.

[12] L. Huang and P. Russer, "Electrically tunable antenna design procedure for mobile applications," *IEEE Transactions on Microwave Theory and Techniques*, vol. 56, no. 12, pp. 2789–2797, 2008.

[13] R. M. C. Cleetus and G. J. Bala, "Frequency reconfigurable antennas: A review," in *2017 International Conference on Signal Processing and Communication (ICSPC)*, IEEE, 2017, pp. 160–164.

[14] A. Horton, S. Chilton, H. Sigmarsson, and J. Ruyle, "Tunable microstrip filter element using magnetically-repositioned ferrofluid load," *Electronics Letters*, vol. 53, no. 4, pp. 256–258, 2017.

[15] A. Horton, P. Winniford, and J. Ruyle, "Frequency and impedance reconfigurable antenna using magnetically-actuated low-loss ferrofluid loads," *Electromagnetics*, vol. 39, no. 8, pp. 594–610, 2019.

[16] A. Dey, R. Guldiken, and G. Mumcu, "Microfluidically reconfigured wideband frequency-tunable liquid-metal monopole antenna," *IEEE Transactions on Antennas and Propagation*, vol. 64, no. 6, pp. 2572–2576, 2016.

[17] C.-T. Chuang and S.-J. Chung, "Synthesis and design of a new printed filtering antenna," *IEEE Transactions on Antennas and Propagation*, vol. 59, no. 3, pp. 1036–1042, 2011.

[18] Y. Yusuf and X. Gong, "Compact low-loss integration of high-Q 3-D filters with highly efficient antennas," *IEEE Transactions on Microwave Theory and Techniques*, vol. 59, no. 4, pp. 857–865, 2011.

[19] Y. Tawk, J. Costantine, and C. Christodoulou, "A varactor-based reconfigurable filtenna," *IEEE Antennas and wireless propagation letters*, vol. 11, pp. 716–719, 2012.

[20] R. E. Lovato, T. Li, and X. Gong, "Tunable filter/antenna integration with bandwidth control," *IEEE Transactions on Microwave Theory and Techniques*, vol. 67, no. 10, pp. 4196–4205, 2019.

[21] W.-J. Wu, Y.-Z. Yin, S.-L. Zuo, Z.-Y. Zhang, and J.-J. Xie, "A new compact filter-antenna for modern wireless communication systems," *IEEE Antennas and Wireless propagation letters*, vol. 10, pp. 1131–1134, 2011.

[22] D. M. Pozar, *Microwave engineering*. John wiley & sons, 2011.

[23] H. T. Friis, "Noise figures of radio receivers," *Proceedings of the IRE*, vol. 32, no. 7, pp. 419–422, 1944.

[24] *Noise figure of passives*, Nov. 2010. [Online]. Available: https://www.microwaves101.com/encyclopedias/noise-figure-of-passives.

[25] S. R. Best, "Realized noise figure of the general receiving antenna," *IEEE Antennas and Wireless Propagation Letters*, vol. 12, pp. 702–705, 2013.

[26] R. W. Irazoqui and C. J. Fulton, "Spatial interference nulling before RF frontend for fully digital phased arrays," *IEEE Access*, vol. 7, pp. 151 261–151 272, 2019.

[27] M. Thibodeau, "Theory, design, and fabrication of frequency agile filtennas," M.S. thesis, University of Oklahoma, 2020.

[28] S. Moon, H. H. Sigmarsson, H. Joshi, and W. J. Chappell, "Substrate integrated evanescent-mode cavity filter with a 3.5 to 1 tuning ratio," *IEEE microwave and wireless components letters*, vol. 20, no. 8, pp. 450–452, 2010.

[29] S. A. Razavi and M. H. Neshati, "Development of a linearly polarized cavity-backed antenna using hmsiw technique," *IEEE Antennas and Wireless Propagation Letters*, vol. 11, pp. 1307–1310, 2012.

[30] K. Schab, L. Jelinek, M. Capek, C. Ehrenborg, D. Tayli, G. A. Vandenbosch, and M. Gustafsson, "Energy stored by radiating systems," *IEEE Access*, vol. 6, pp. 10 553–10 568, 2018.

[31] M. Capek, L. Jelinek, K. Schab, M. Gustafsson, B. L. G. Jonsson, F. Ferrero, and C. Ehrenborg, "Optimal planar electric dipole antennas: Searching for antennas reaching the fundamental bounds on selected metrics," *IEEE Antennas and Propagation Magazine*, vol. 61, no. 4, pp. 19–29, 2019.

[32] Y. Yusuf and X. Gong, "A vertical integration of high-Q filters with patch antennas with enhanced bandwidth and high efficiency," in *2011 IEEE MTT-S International Microwave Symposium*, IEEE, 2011, pp. 1–4.

[33] M. Gustafsson and B. L. G. Jonsson, "Antenna Q and stored energy expressed in the fields, currents, and input impedance," *IEEE Transactions on Antennas and Propagation*, vol. 63, no. 1, pp. 240–249, 2014.

[34] A. D. Yaghjian and S. R. Best, "Impedance, bandwidth, and Q of antennas," *IEEE Transactions on Antennas and Propagation*, vol. 53, no. 4, pp. 1298–1324, 2005.